Lepton *CP* violation in a ν2HDM with flavor

E. Barradas-Guevara,[1,2,*] O. Félix-Beltrán,[3,2,†] F. Gonzalez-Canales,[3,2,‡] and M. Zeleny-Mora[1,2,§]

[1]*Facultad de Ciencias Físico Matemáticas, Benemérita Universidad Autónoma de Puebla, Apdo. Postal 1152, Puebla, Pue. 72000, México*

[2]*Centro Internacional de Física Fundamental (CIFFU), Benemérita Universidad Autónoma de Puebla, Apdo. Postal 1152, Puebla, Pue. 72000, México*

[3]*Facultad de Ciencias de la Electrónica, Benemérita Universidad Autónoma de Puebla, Apdo. Postal 542, Puebla, Pue. 72000, México*

(Received 20 April 2017; published 2 February 2018)

In this work we propose an extension to the Standard Model in which we consider a type-III two-Higgs-doublet model (2HDM) plus massive neutrinos and the horizontal flavor symmetry S_3 (ν2HDM $\otimes$ S_3). In the above framework and with the explicit breaking of flavor symmetry S_3, the Yukawa matrices in the flavor-adapted basis are represented by means of a matrix with two texture zeros. Also, the active neutrinos are considered as Majorana particles and their masses are generated through the type-I seesaw mechanism. The unitary matrices that diagonalize the mass matrices, as well as the flavor-mixing matrices, are expressed in terms of fermion mass ratios. Consequently, in the mass basis the entries of the Yukawa matrices naturally acquire the form of the so-called *Cheng-Sher ansatz*. For the leptonic sector of ν2HDM $\otimes$ S_3, we compare, through a χ^2 likelihood test, the theoretical expressions of the flavor-mixing angles with the masses and flavor-mixing leptons current experimental data. The results obtained in this χ^2 analysis are in very good agreement with the current experimental data. We also obtain allowed value ranges for the "Dirac-like" phase factor, as well as for the two Majorana phase factors. Furthermore, we study the phenomenological implications of these numerical values of the *CP*-violation phases on the neutrinoless double-beta decay, and for long baseline neutrino oscillation experiments such as T2K, NOνA, and DUNE.

DOI: 10.1103/PhysRevD.97.035003

I. INTRODUCTION

According to the most recent neutrino physics literature [1,2], there are still several unresolved issues, including whether the neutrinos are Dirac or Majorana fermions, the absolute neutrino mass scale, and the possible sources of charge-parity (*CP*) violation (CPV) in leptons. Nowadays, answers to these questions are being investigated via the experimental results concerning KamLAND reactor neutrinos [3–5] in the current high-statistics short-baseline reactor neutrino experiments RENO [6,7], Double Chooz [8], and Daya Bay [9]. Also, one of the most interesting effects related to neutrino oscillation in matter is that these periodic transformations of neutrinos from one flavor to another can induce a fake *CP*-violating effect. Therefore, the long-baseline (LBL) neutrino oscillation experiments are good candidates for determining the "Dirac-like" *CP* violation phase as well as resolving the mass hierarchy problem [10]. The recent measurements reported by the T2K [11–14], NOνA [15,16] and Super-Kamiokande experiments [17] suggest a nearly maximal *CP* violation. In these experiments the "Dirac-like" *CP* phase takes the value $\delta_{CP} \simeq 3\pi/2$, with a statistical significance below the 3σ level. Moreover, the data obtained in the global fits of neutrino oscillations agree with a nonzero δ_{CP} phase, whereby the previous value is confirmed [2,18–21].

The concepts of flavor and mass generation are strongly intertwined. In order to know the flavor dynamics in models beyond the Standard Model (SM), we need to understand the mechanism of flavor and mass generation arising in the standard theory. In the latter, the Yukawa matrices are of great interest because their eigenvalues define the fermion masses. Moreover, for multi-Higgs models, flavor-changing neutral current (FCNCs) arise naturally from the inability to simultaneously diagonalize the mass and Yukawa matrices. In particular, models like the type-III two-Higgs-doublet model (2HDM-III), in which the two Higgs doublets are coupled to all fermions, allow the presence of FCNCs at tree level mediated by the

*barradas@fcfm.buap.mx
†olga.felix@correo.buap.mx
‡felixfcoglz@gmail.com
§moiseszeleny@gmail.com

Higgs [22–27]. The 2HDM predicts three neutral states $H^0_{1,2,3}$ and a pair of charged states denoted as $H^{\pm}_{1,2}$ [28,29]. The Higgs-fermion couplings ($H^0\bar{f}f$) in the 2HDM are given as [22,23,25–27]

$$\mathcal{L}_Y = \bar{f}_i(S_{ij} + \gamma^5 P_{ij}) f_j H^0_a, \qquad (a = 1, 2, 3). \quad (1)$$

In 2HDM-III the FCNCs are kept under control by imposing some texture zeros in the Yukawa matrices. This fact reproduces the observed fermion masses and mixing angles [30]. Using texture shapes allows a direct relation between the Yukawa matrix entries and the parameters used to compute the decay widths and cross section, without losing the terms proportional to the light fermion masses. Specifically, considering a zero-texture Yukawa matrix, one obtains the *Cheng-Sher ansatz* for flavor mixing couplings (widely used in the literature) where flavored couplings are considered proportional to the involved fermion masses [31].

The matter content in the 2HDM is divided among the quark and lepton sectors. In turn, these sectors are subdivided into two sectors: up- and down-type quarks in the quarks sector, and charged leptons and neutrinos in the leptons sector. The fermions in each of these subsectors are analogous to each other because they have completely identical couplings to all gauge bosons, although their masses are not the same. Therefore, before spontaneous symmetry breaking (SSB), the Yukawa Lagrangian in the above subsectors is invariant under permutations of flavor indices. In other words, each of these subsectors is invariant under the action of a S_3 symmetry group. This symmetry group has only three irreducible representations that correspond to two singlets and a doublet [32,33].

On the other hand, the mass spectrum for Dirac fermions obtained from the experimental data obeys the following strong hierarchy [34]:

$$\begin{aligned} &\hat{m}_e \sim 10^{-6}, \quad \hat{m}_\mu \sim 10^{-3}, \quad \hat{m}_\tau \sim 1, \\ &\hat{m}_u \sim 10^{-5}, \quad \hat{m}_c \sim 10^{-3}, \quad \hat{m}_t \sim 1, \\ &\underbrace{\hat{m}_d \sim 10^{-3}, \quad \hat{m}_s \sim 10^{-2},}_{\mathbf{2}} \quad \underbrace{\hat{m}_b \sim 1.}_{\mathbf{1}} \end{aligned} \quad (2)$$

In the above expression $\hat{m}_l = m_l/m_\tau$ ($l = e, \mu, \tau$) stands for charged leptons, $\hat{m}_U = m_U/m_t$ ($U = u, c, t$) stands for up-type quarks, and $\hat{m}_D = m_D/m_b$ ($D = d, s, b$) stands for down-type quarks. The behavior of these mass ratios in terms of irreducible representations of some symmetry group can be interpreted as follows: the two lighter particles are associated with a doublet representation **2**, whereas the heaviest particle is assigned a singlet representation **1**. The smallest non-Abelian group with irreducible singlet and doublet representations is the group of permutations of three objects. Hence, we expect the hierarchical nature of the Dirac fermion mass matrices to have its origin in the representation structure $\mathbf{3} = \mathbf{2} \oplus \mathbf{1}$ of S_3. In the theoretical framework of the SM, as well as for the 2HDM, the neutrinos are massless particles, a fact that is in disagreement with the results obtained in the neutrino oscillation experiments.

Therefore, in this work we will study the flavor dynamics through Yukawa matrices in the specific scenario of 2HDM-III plus massive neutrinos and a horizontal flavor symmetry S_3 (ν2HDM $\otimes$ S_3). In this context, under the action of the S_3 flavor symmetry group the right-handed neutrinos as well as the two Higgs fields transform as singlets, while the active neutrinos are considered as Majorana particles and their masses are generated through the type-I seesaw mechanism. Hence, it is necessary to consider the following hybrid mass term, which involves the Dirac and Majorana neutrino mass terms [35]:

$$\mathcal{L}_{\mathrm{M+D}} = -\frac{1}{2}\bar{\eta}_L \mathbf{M}_{\mathrm{M+D}} (\eta_L)^c + \mathrm{H.c.}, \quad (3)$$

where $\eta = (\nu_L, (N_R)^c)^\top$ and

$$\mathbf{M}_{\mathrm{M+D}} = \begin{pmatrix} \mathbf{0} & \mathbf{M}_{\nu_D} \\ \mathbf{M}^\top_{\nu_D} & \mathbf{M}_R \end{pmatrix}. \quad (4)$$

In the above expression, $\mathbf{M}_{\nu_D}$ and $\mathbf{M}_R$ are the Dirac and right-handed neutrino mass matrices, respectively. In the special limit $\mathbf{M}_R \gg \mathbf{M}_{\nu_D}$, the effective mass matrix of left-handed neutrinos is given by the type-I seesaw mechanism whose expression is[1]

$$\mathbf{M}_\nu = \mathbf{M}_{\nu_D} \mathbf{M}_R^{-1} \mathbf{M}^\top_{\nu_D}. \quad (5)$$

If the fermion mass matrices do not have any element equal to zero, on the one hand, the mass matrix of active neutrinos has 12 free parameters, since $\mathbf{M}_\nu$ is a complex symmetric matrix because this matrix comes from a Majorana mass term. On the other hand, the Dirac fermion mass matrices do not have any special features, i.e., these matrices are not Hermitian or symmetric. This is mainly due to the fact that the Yukawa matrices are represented through a 3×3 complex matrix. Hence, for Dirac mass matrices we have 18 free parameters.

After the explicit sequential breaking of flavor symmetry according to the chain $S^{\mathrm{j}}_{3L} \otimes S^{\mathrm{j}}_{3R} \supset S^{\mathrm{diag}}_3 \supset S^{\mathrm{diag}}_2$, all Yukawa matrices in the flavor-adapted basis are represented by means of a matrix with two texture zeros. Therefore, all fermion mass matrices in the model have the same generic form with two texture zeros.

The difference between the 2HDM and ν2HDM $\otimes$ S_3 lies in the Yukawa structure, the symmetries of the Higgs sector, and the possible appearance of new CPV sources.

[1]The implications of heavy Majorana neutrinos at the LHC was analyzed in Refs. [36,37].

This CPV can arise from the same phase appearing in the Cabibbo-Kobayashi matrix as in the SM, or some extra phase which arises from the Yukawa field or from the Higgs potential, either explicitly or spontaneously. The Higgs potential preserves *CP* symmetry, whereby CPV comes from the Yukawa matrices.

In order to validate our hypothesis where the S_3 horizontal flavor symmetry is explicitly broken, and hence all fermion mass matrices are represented through a matrix with two texture zeros, we make a likelihood test where the χ^2 function is defined in terms of leptonic flavor-mixing angles. Afterwards, we shall investigate the phenomenological implications of these results on neutrinoless double-beta decay and CPV in neutrino oscillations in matter.

The organization of this work is as follows. In Sec. II we present the Yukawa Lagrangian in the ν2HDM $\otimes$ S_3, and the form of the Dirac and Majorana fermion mass matrices in terms of its eigenvalues. In this way, we derive explicit and analytical expressions for the leptonic flavor-mixing angles and Higgs-fermion couplings. In Sec. III we present a detailed likelihood test where the χ^2 function is defined in terms of leptonic mixing angles. In Sec. IV we explore the phenomenological implications of the numerical values obtained for the *CP*-violating phase factors on neutrinoless double-beta decay and neutrino oscillations in matter. Finally, in Sec. V we present our conclusions about the present work.

II. THE YUKAWA LAGRANGIAN IN THE ν2HDM $\otimes$ S_3

In the fermion matter content of the SM (which is the same as that for the 2HDM), there are no right-handed neutrinos; consequently, in both models a neutrino mass term is not allowed. This latter fact gainsays the results obtained in the neutrino oscillation experiments which requires neutrinos to have nonzero masses [34]. In order to include a Majorana neutrino mass term in the 2HDM, we need to increase its matter content. For this reason, we consider six neutrino fields: three left-handed $\nu_L = (\nu_{eL}, \nu_{\mu L}, \nu_{\tau L})^\top$ and three right-handed $N_R = (N_{1R}, N_{2R}, N_{3R})^\top$. The right-handed neutrinos must be uncharged under the weak and electromagnetic interactions, which means that this kind of neutrinos are singlets under $G_{\rm EW} \equiv SU(2)_L \otimes U(1)_Y$. In other words, only the left-handed neutrinos take part in the electroweak interaction. In this theoretical framework, we have all SM matter content plus massive neutrinos and an extra Higgs boson, whereby it is called the ν2HDM. In the weak basis, the Yukawa interaction Lagrangian for Dirac fermions in the ν2HDM is given by [29,38,39]

$$\mathcal{L}_{\rm Y}^{\rm w} = \sum_{k=1}^{2} (\mathbf{Y}_k^{{\rm w},u} \bar{Q} \tilde{\Phi}_k u_R + \mathbf{Y}_k^{{\rm w},d} \bar{Q} \Phi_k d_R + \mathbf{Y}_k^{{\rm w},\nu_D} \bar{L} \tilde{\Phi}_k N_R + \mathbf{Y}_k^{{\rm w},l} \bar{L} \Phi_k l_R) + {\rm H.c.}, \quad (6)$$

where $Q = (u, d)_L^\top$ and $L = (\nu_l, l)_L^\top$ are the left-handed doublets of $SU(2)_L$; u_R, d_R, and l_R are the right-handed singlets of the electroweak gauge group. In this expression, the superscript "w" indicates that we are working in the weak basis, while the indices l, u, and d represent the charged leptons, and u- and d-type quarks, respectively. Also, $\Phi_k = (\phi_k^+, \phi_k^0)^\top$ denotes the two Higgs fields which are doublets of $SU(2)_L$, with $\tilde{\Phi}_k = i\sigma_2 \Phi_k^*$. Finally, the $\mathbf{Y}_k^{{\rm w},{\rm j}}$ are the Yukawa matrices in the weak basis, where the ${\rm j}$ superscript denotes the Dirac fermions, (${\rm j} = u, d, l, \nu_D$) [29]. In general, after the SSB and in the context of the ν2HDM, the Dirac fermion mass matrix in the weak basis can be written as [29,38,40]

$$\mathbf{M}_{\rm j}^{\rm w} = \frac{1}{\sqrt{2}} \sum_{k=1}^{2} v_k \mathbf{Y}_k^{{\rm w},{\rm j}}, \quad (7)$$

where v_k are the vacuum expectation values of the two Higgs bosons Φ_k, with $k = 1, 2$.

A. Mass matrices from the S_3 flavor symmetry

To reduce the free parameters in the fermion mass matrices, we will consider a horizontal symmetry which correlates the particle flavor indices with each other; thus, the Yukawa matrices could be represented by means of a 3×3 Hermitian matrix. Consequently, for three families or generations of quarks and leptons, we propose[2] that after the SSB, the Yukawa Lagrangian in the ν2HDM presents the permutation group S_3 as a horizontal flavor symmetry. In this context, the right-handed neutrinos, as well as the two Higgs bosons, transform as singlets under the action of S_3 flavor symmetry. In other words, the right-handed neutrinos and the two scalar fields Φ_k are flavorless particles, whereby these fields are treated as scalars with respect to the S_3 symmetry transformations. The general way to implement the flavor symmetry is by considering that under the action of S_3 symmetry, the left- and right-handed spinors transform as [42]

$$\psi_{{\rm j}L}^{\rm s} = \mathbf{g}_{\rm a}^{\rm j} \psi_{{\rm j}L} \quad \text{and} \quad \psi_{{\rm j}R}^{\rm s} = \tilde{\mathbf{g}}_{\rm b}^{\rm j} \psi_{{\rm j}R}, \qquad {\rm a, b} = 1, \ldots, 6. \quad (8)$$

At this point, the proposed flavor symmetry for the Yukawa Lagrangian is the $S_{3L}^{\rm j} \otimes S_{3R}^{\rm j}$ group, whose elements are the pairs $(\mathbf{g}_{\rm a}^{\rm j}, \tilde{\mathbf{g}}_{\rm b}^{\rm j})$, where $\mathbf{g}_{\rm a}^{\rm j} \in S_{3L}^{\rm j}$ and $\tilde{\mathbf{g}}_{\rm b}^{\rm j} \in S_{3R}^{\rm j}$, while the superscript "s" means that fields are in the flavor-symmetry-adapted basis. However, the mass terms $\mathcal{L}_m \sim \bar{\psi}_{{\rm j}L} \mathbf{M}_{\rm j} \psi_{{\rm j}R}$ and charged currents $\mathcal{J}_\mu \sim \bar{\psi}_{{\rm j}L} \gamma_\mu \psi_{{\rm j}L} W^\mu$ in the Lagrangian are not invariant under the $S_{3L}^{\rm j} \otimes S_{3R}^{\rm j}$ group. In order to make $\mathcal{L}_m$ and $\mathcal{J}_\mu$ invariant under the flavor group transformations, the elements of the

[2] As other authors have done in the SM [41–43] (and references therein).

$S_{3L}^{\mathrm{j}} \otimes S_{3R}^{\mathrm{j}}$ group must satisfy the relation $\mathbf{g}_{\mathrm{a}} \equiv \mathbf{g}_{\mathrm{a}}^{\mathrm{j}} = \tilde{\mathbf{g}}_{\mathrm{b}}^{\mathrm{j}}$. The latter condition implies that the flavor group is reduced according to the chain $S_{3L}^{\mathrm{j}} \otimes S_{3R}^{\mathrm{j}} \supset S_3^{\mathrm{diag}}$ [42]. This flavor-symmetry-breaking chain should be interpreted as meaning that all fermions in the model must be transformed with the same flavor group and the same element thereof. In the above, the flavor group is called S_3^{diag} because its elements are the pairs $(\mathbf{g}_{\mathrm{a}}, \mathbf{g}_{\mathrm{a}})$, where $\mathbf{g}_{\mathrm{a}} \in S_{3L}$ [42].

Finally, it is easy conclude that S_3^{diag} is the horizontal flavor symmetry which conserves the invariance of $\mathcal{L}_{\mathrm{Y}}^{\mathrm{w}}$ under the action of the electroweak gauge group. Also, from the invariance of $\mathcal{L}_m$ under the action of the S_3^{diag} group, we obtain that fermion mass matrices commute with all elements of the flavor group.

In the weak basis, the two Yukawa matrices in Eq. (7) are represented by means of a matrix with the exact S_3^{diag} symmetry. Therefore, these Yukawa matrices are expressed as

$$\mathbf{Y}_k^{\mathrm{w,j}} \equiv \mathbf{Y}_k^{\mathrm{j}3} = \alpha_k^{\mathrm{j}} \mathbf{P_1}, \tag{9}$$

where α_k^{j} are real constants associated with the flavor symmetry. The explicit form of the matrix $\mathbf{P_1}$ is given by Eq. (A2), and corresponds to the projector associated with the symmetric singlet representation of S_3. Hence, the Dirac fermion mass matrix is

$$\mathbf{M}_{\mathrm{j}}^{\mathrm{w}} = \frac{1}{\sqrt{2}} \sum_{k=1}^{2} v_k \mathbf{Y}_k^{\mathrm{j}3} = m_{\mathrm{j}3} \mathbf{P_1}, \tag{10}$$

where $m_{\mathrm{j}3} = \frac{1}{\sqrt{2}}(v_1 \alpha_1^{\mathrm{j}} + v_2 \alpha_2^{\mathrm{j}})$. In the flavor-adapted basis, the Dirac fermion mass matrices are [40]

$$\mathbf{M}_{\mathrm{j}}^{\mathrm{s}} = \mathbf{U}_{\mathrm{s}}^{\dagger} \mathbf{M}_{\mathrm{j}}^{\mathrm{w}} \mathbf{U}_{\mathrm{s}} = m_{\mathrm{j}3} \mathbf{U}_{\mathrm{s}}^{\dagger} \mathbf{P_1} \mathbf{U}_{\mathrm{s}} = \mathrm{diag}(0, 0, m_{\mathrm{j}3}), \tag{11}$$

where

$$\mathbf{U}_{\mathrm{s}} = \frac{1}{\sqrt{6}} \begin{pmatrix} \sqrt{3} & 1 & \sqrt{2} \\ -\sqrt{3} & 1 & \sqrt{2} \\ 0 & -2 & \sqrt{2} \end{pmatrix}. \tag{12}$$

The interpretation of Eq. (11) is that under an exact S_3^{diag} symmetry, the mass spectrum for Dirac fermions consists of a massive particle and two massless particles [44]. The only massive particle in each fermion mass spectrum corresponds to the heaviest fermion. However, this result disagrees with the experimental data on quark and lepton masses [34].

Since the two Higgs fields are invariant under flavor symmetry transformations, these are naturally assigned to S_3 flavor singlets. If the Yukawa Lagrangian is exactly invariant under S_3 flavor transformations, the two scalar fields can only couple with the S_3-singlet component of fermion fields. Consequently, only the S_3-singlet component of fermion fields acquires a nonzero mass. As the third family is the heaviest, here we assign the fermion fields in the third family to the singlet irreducible representation of S_3.

So, with the aim to generate a nonzero mass for all fermions in the model, here we will break the flavor symmetry in an explicitly sequential way, according to the chain $S_{3L}^{\mathrm{j}} \otimes S_{3R}^{\mathrm{j}} \supset S_3^{\mathrm{diag}} \supset S_2^{\mathrm{diag}}$. The first two fermion families and the third one are assigned to the doublet and singlet irreducible representations of S_3^{diag}, respectively. The mass of the second fermion family is generated when the S_3^{diag} flavor symmetry is explicitly broken into the S_2^{diag} group. This symmetry breaking is carried out when we add the following term to the $\mathbf{Y}_k^{\mathrm{j}3}$ matrix in Eq. (9):

$$\mathbf{Y}_k^{\mathrm{j}2} = \beta_k^{\mathrm{j}} \mathbf{T}_{z1}^{+} + \gamma_k^{\mathrm{j}} \mathbf{T}_{z2}^{+}, \tag{13}$$

where β_k^{j} and γ_k^{j} are real constant parameters. The explicit form of the tensors $\mathbf{T}_{z1}^{+}$ and $\mathbf{T}_{z2}^{+}$ is given by Eq. (A10). The $\mathbf{Y}_k^{\mathrm{j}2}$ matrix mixes the symmetric component of the doublet with the singlet. Finally, the first fermion family's mass is generated by adding the term

$$\mathbf{Y}_k^{\mathrm{j}1} = \epsilon_k^{\mathrm{j}} \mathbf{T}_x^{+} + \rho_k^{\mathrm{j}} \mathbf{T}_x^{-} \tag{14}$$

to the matrices in Eqs. (9) and (14), where ϵ_k^{j} and ρ_k^{j} are real constant parameters. Thus, the explicit form of the tensors $\mathbf{T}_x^{+}$ and $\mathbf{T}_x^{-}$ is given by Eq. (A4). The $\mathbf{Y}_k^{\mathrm{j}1}$ matrix mixes the components of the doublet representation with each other in the weak basis. So, in the weak basis and under the explicit sequential breaking of flavor symmetry according to the chain $S_{3L}^{\mathrm{j}} \otimes S_{3R}^{\mathrm{j}} \supset S_3^{\mathrm{diag}} \supset S_2^{\mathrm{diag}}$, we obtain the Yukawa matrices which produce three massive fermions. These Yukawa matrices are the sum of the three expressions given by Eqs. (9), (13), and (14). Then,

$$\begin{aligned} \mathbf{Y}_k^{\mathrm{w,j}} &= \mathbf{Y}_k^{\mathrm{j}3} + \mathbf{Y}_k^{\mathrm{j}2} + \mathbf{Y}_k^{\mathrm{j}1} \\ &= \alpha_k^{\mathrm{j}} \mathbf{P_1} + \beta_k^{\mathrm{j}} \mathbf{T}_{z1}^{+} + \gamma_k^{\mathrm{j}} \mathbf{T}_{z2}^{+} + \epsilon_k^{\mathrm{j}} \mathbf{T}_x^{+} + \rho_k^{\mathrm{j}} \mathbf{T}_x^{-}, \mathbf{Y}_k^{\mathrm{w,j}} \\ &= \begin{pmatrix} e_k^{\mathrm{w,j}} & a_k^{\mathrm{w,j}} & f_k^{\mathrm{w,j}} \\ a_k^{\mathrm{w,j}*} & b_k^{\mathrm{w,j}} & c_k^{\mathrm{w,j}} \\ f_k^{\mathrm{w,j}*} & c_k^{\mathrm{w,j}*} & d_k^{\mathrm{w,j}} \end{pmatrix}, \end{aligned} \tag{15}$$

where

$$\begin{aligned} a_k^{\mathrm{w,j}} &= \frac{\alpha_k^{\mathrm{j}} + 3(\beta_k^{\mathrm{j}} + i\rho_k^{\mathrm{j}})}{3}, \quad b_k^{\mathrm{w,j}} = \frac{\alpha_k^{\mathrm{j}} + 3(\beta_k^{\mathrm{j}} + \epsilon_k^{\mathrm{j}})}{3}, \\ c_k^{\mathrm{w,j}} &= \frac{\alpha_k^{\mathrm{j}} + 3(\gamma_k^{\mathrm{j}} - \epsilon_k^{\mathrm{j}} + i\rho_k^{\mathrm{j}})}{3}, \quad d_k^{\mathrm{w,j}} = \frac{\alpha_k^{\mathrm{j}} - 6\beta_k^{\mathrm{j}}}{3}, \\ e_k^{\mathrm{w,j}} &= \frac{\alpha_k^{\mathrm{j}} + 3(\beta_k^{\mathrm{j}} - \epsilon_k^{\mathrm{j}})}{3}, \quad f_k^{\mathrm{w,j}} = \frac{\alpha_k^{\mathrm{j}} + 3(\gamma_k^{\mathrm{j}} + \epsilon_k^{\mathrm{j}} - i\rho_k^{\mathrm{j}})}{3}. \end{aligned} \tag{16}$$

In this same basis, now the fermion mass matrices $\mathbf{M}_{\mathrm{j}}^{\mathrm{w}}$ take the form

$$\mathbf{M}_{\mathrm{j}}^{\mathrm{w}} = \frac{1}{\sqrt{2}}\sum_{k=1}^{2} v_k \mathbf{Y}_k^{\mathrm{w,j}} = \frac{1}{\sqrt{2}}\sum_{k=1}^{2} v_k(\alpha_k^{\mathrm{j}}\mathbf{P_1} + \beta_k^{\mathrm{j}}\mathbf{T}_{z1}^{+} + \gamma_k^{\mathrm{j}}\mathbf{T}_{z2}^{+} + \epsilon_k^{\mathrm{j}}\mathbf{T}_{x}^{+} + \rho_k^{\mathrm{j}}\mathbf{T}_{x}^{-}). \tag{17}$$

Thus, with the help of the previous expression and Eq. (15), it is easy to conclude that the Dirac fermion mass matrices are Hermitian matrices that do not have any element equal to zero. However, in the flavor-adapted basis the mass matrices in Eq. (17) acquire the following form:

$$\begin{aligned}
\mathbf{M}_{\mathrm{j}}^{\mathrm{s}} &= \mathbf{U}_{\mathrm{s}}^{\dagger}\mathbf{M}_{\mathrm{j}}^{\mathrm{w}}\mathbf{U}_{\mathrm{s}} = \frac{1}{\sqrt{2}}\sum_{k=1}^{2} v_k \mathbf{U}_{\mathrm{s}}^{\dagger}\mathbf{Y}_k^{\mathrm{w,j}}\mathbf{U}_{\mathrm{s}},\\
\mathbf{M}_{\mathrm{j}}^{\mathrm{s}} &= \mathbf{P}_{\mathrm{j}}\begin{pmatrix} 0 & |A_{\mathrm{j}}| & 0 \\ |A_{\mathrm{j}}| & B_{\mathrm{j}} & C_{\mathrm{j}} \\ 0 & C_{\mathrm{j}} & D_{\mathrm{j}} \end{pmatrix}\mathbf{P}_{\mathrm{j}}^{\dagger}\\
&= \frac{v\cos\beta}{\sqrt{2}}\times\left[\begin{pmatrix} 0 & A_1^{\mathrm{j}} & 0 \\ A_1^{\mathrm{j}*} & B_1^{\mathrm{j}} & C_1^{\mathrm{j}} \\ 0 & C_1^{\mathrm{j}} & D_1^{\mathrm{j}} \end{pmatrix}\right.\\
&\quad \left. + \tan\beta\begin{pmatrix} 0 & A_2^{\mathrm{j}} & 0 \\ A_2^{\mathrm{j}*} & B_2^{\mathrm{j}} & C_2^{\mathrm{j}} \\ 0 & C_2^{\mathrm{j}} & D_2^{\mathrm{j}} \end{pmatrix}\right],
\end{aligned} \tag{18}$$

where $\mathbf{P}_{\mathrm{j}} = \mathrm{diag}(1, e^{-i\phi_{\mathrm{j}}}, e^{-i\phi_{\mathrm{j}}})$ with $\phi_{\mathrm{j}} = \arg\{A_{\mathrm{j}}\}$, and

$$\begin{aligned}
A_k^{\mathrm{j}} &= -\sqrt{3}(\epsilon_k^{\mathrm{j}} - i\rho_k^{\mathrm{j}}), \qquad B_k^{\mathrm{j}} = -\frac{2}{3}(\beta_k^{\mathrm{j}} + 2\gamma_k^{\mathrm{j}}),\\
C_k^{\mathrm{j}} &= \frac{\sqrt{2}}{3}(4\beta_k^{\mathrm{j}} - \gamma_k^{\mathrm{j}}), \qquad D_k^{\mathrm{j}} = \alpha_k^{\mathrm{j}} + \frac{2}{3}(\beta_k^{\mathrm{j}} + 2\gamma_k^{\mathrm{j}}),
\end{aligned} \tag{19}$$

with $k = 1, 2$. The parameters in Eq. (19) are the Yukawa matrix elements expressed in the flavor-adapted basis. Finally, in the Higgs sector, $\tan\beta = \frac{v_2}{v_1}$ with $v^2 = v_1^2 + v_2^2 = (246.22\ \mathrm{GeV})^2$.

Here, we consider that the active neutrinos acquire their masses through the type-I seesaw mechanism [Eq. (5)], where the Dirac fermion mass matrix is given by Eq. (18), while we suppose that in the flavor-adapted basis the right-handed neutrino mass matrix has the form

$$\mathbf{M}_R^{\mathrm{s}} = \mathrm{diag}(A_R, A_R, D_R)\mathbf{D}^{(3)}(A_1). \tag{20}$$

In the latter expression, A_R and D_R are real parameters, and the form of the matrix $\mathbf{D}^{(3)}(A_1)$ is given by Eq. (A1). So, in the flavor-adapted basis the active neutrino mass matrix is

$$\mathbf{M}_\nu^{\mathrm{s}} = \mathbf{P}_\nu^{\dagger}\begin{pmatrix} 0 & a_\nu & 0 \\ a_\nu & |b_\nu| & |c_\nu| \\ 0 & |c_\nu| & d_\nu \end{pmatrix}\mathbf{P}_\nu^{\dagger}, \tag{21}$$

where $\mathbf{P}_\nu = e^{i\phi_\nu}\mathrm{diag}(1, e^{-i2\phi_\nu}, e^{-i\phi_\nu})$ with $\phi_\nu = \arg\{C_\nu\}$, and $\arg\{C_\nu\} = 2\arg\{B_\nu\}$,

$$\begin{aligned}
a_\nu &= \frac{|A_{\nu_D}|^2}{A_R}, \qquad b_\nu = \frac{C_{\nu_D}^2}{D_R} + \frac{2B_{\nu_D}A_{\nu_D}^*}{A_R},\\
c_\nu &= \frac{C_{\nu_D}D_{\nu_D}}{D_R} + \frac{C_{\nu_D}A_{\nu_D}^*}{A_R}, \quad \text{and} \quad d_\nu = \frac{D_{\nu_D}^2}{D_R}.
\end{aligned} \tag{22}$$

In this work, we study the flavor dynamics through the Yukawa matrices in the 2HDM-III plus massive neutrinos and with a horizontal flavor symmetry S_3. This theoretical framework is called ν2HDM $\otimes$ S_3.

B. The mass and mixing matrices as functions of fermion masses

For a normal [inverted] hierarchy[3] in the mass spectrum, the real symmetric matrices in Eqs. (18) and (21)—which are associated with the fermion mass matrices—can be reconstructed through the orthogonal transformation[4]

$$\bar{\mathbf{M}}_f^{\mathrm{n[i]}} = m_{f3[2]}\mathbf{O}_f^{\mathrm{n[i]}}\Delta_f^{\mathrm{n[i]}}(\mathbf{O}_f^{\mathrm{n[i]}})^{\top}, \qquad f = u, d, l, \nu, \tag{23}$$

where $\mathbf{\Delta}_f^{\mathrm{n[i]}} = \mathrm{diag}(\hat{m}_{f1[3]}, -\hat{m}_{f2[1]}, 1)$; in this expression $\hat{m}_{f1[3]} = m_{f1[3]}/m_{f3[2]}$ and $\hat{m}_{f2[1]} = |m_{f2[1]}|/m_{f3[2]}$. Here, $m_{f2[1]} = -|m_{f2[1]}|$ and the m_f's are the eigenvalues of the fermion mass matrices, i.e., the particle masses. From algebraic invariants of the expression in Eq. (23) we have

$$\begin{aligned}
a_f^{\mathrm{n[i]}} &\equiv \frac{(\mathbf{M}_f)_{12}}{m_{f3[2]}} = \sqrt{\frac{\hat{m}_{f1[3]}\hat{m}_{f2[1]}}{1-\delta_f}},\\
b_f^{\mathrm{n[i]}} &\equiv \frac{(\mathbf{M}_f)_{22}}{m_{f3[2]}} = \hat{m}_{f1[3]} - \hat{m}_{f2[1]} + \delta_f,\\
c_f^{\mathrm{n[i]}} &\equiv \frac{(\mathbf{M}_f)_{23}}{m_{f3[2]}} = \sqrt{\frac{\delta_f}{1-\delta_f}\xi_{f1[3]}\xi_{f2[1]}},\\
d_f^{\mathrm{n[i]}} &\equiv \frac{(\mathbf{M}_f)_{33}}{m_{f3[2]}} = 1 - \delta_f,
\end{aligned} \tag{24}$$

where $\xi_{f1[3]} = 1 - \hat{m}_{f1[3]} - \delta_f$ and $\xi_{f2[1]} = 1 + \hat{m}_{f2[1]} - \delta_f$. Also, the free parameter δ_f must satisfy the relation $1 - \hat{m}_{f1[3]} > \delta_f > 0$ [41]. The real orthogonal matrix given in Eq. (23) written in terms of fermion masses has the form [38,43]

[3]The inverted hierarchy is only valid for neutrinos.

[4]The superscripts "n" and "[i]" denote the normal and inverted hierarchies in the neutrino mass spectrum.

$$\mathbf{O}_f^{\mathrm{n[i]}} = \begin{pmatrix} \sqrt{\frac{\hat{m}_{f2[1]}\xi_{f1[3]}}{\mathcal{D}_{f1[3]}}} & -\sqrt{\frac{\hat{m}_{f1[3]}\xi_{f2[1]}}{\mathcal{D}_{f2[1]}}} & \sqrt{\frac{\hat{m}_{f1[3]}\hat{m}_{f2[1]}\delta_f}{\mathcal{D}_{f3[2]}}} \\ \sqrt{\frac{\hat{m}_{f1[3]}(1-\delta_f)\xi_{f1[3]}}{\mathcal{D}_{f1[3]}}} & \sqrt{\frac{\hat{m}_{f2[1]}(1-\delta_f)\xi_{f2[1]}}{\mathcal{D}_{f2[1]}}} & \sqrt{\frac{\delta_f(1-\delta_f)}{\mathcal{D}_{f3[2]}}} \\ -\sqrt{\frac{\hat{m}_{f1[3]}\delta_f\xi_{f2[1]}}{\mathcal{D}_{f1[3]}}} & -\sqrt{\frac{\hat{m}_{f2[1]}\delta_f\xi_{f1[3]}}{\mathcal{D}_{f2[1]}}} & \sqrt{\frac{\xi_{f1[3]}\xi_{f2[1]}}{\mathcal{D}_{f3[2]}}} \end{pmatrix}. \tag{25}$$

In this orthogonal matrix we have

$$\begin{aligned} \mathcal{D}_{f1[3]} &= (1-\delta_f)(\hat{m}_{f1[3]} + \hat{m}_{f2[1]})(1-\hat{m}_{f1[3]}), \\ \mathcal{D}_{f2[1]} &= (1-\delta_f)(\hat{m}_{f1[3]} + \hat{m}_{f2[1]})(1+\hat{m}_{f2[1]}), \\ \mathcal{D}_{f3[2]} &= (1-\delta_f)(1-\hat{m}_{f1[3]})(1+\hat{m}_{f2[1]}). \end{aligned} \tag{26}$$

In the theoretical framework of ν2HDM $\otimes S_3$, the unitary matrices that diagonalize the mass matrices of charged leptons and active neutrinos are defined as

$$\mathbf{U}_\ell^{\mathrm{n[i]}} = \mathbf{U}_{\mathrm{s}}\mathbf{P}_\ell\mathbf{O}_\ell^{\mathrm{n[i]}}, \qquad \ell = l, \nu. \tag{27}$$

The matrix $\mathbf{U}_{\mathrm{s}}$ is given by Eq. (12), and the diagonal phase matrices can be found in Eqs. (18) and (21). Finally, the real orthogonal matrix $\mathbf{O}_\ell^{\mathrm{n[i]}}$ is given in Eq. (25). From the previous unitary matrix, in the mass basis, the Dirac fermion mass matrices take the form

$$\begin{aligned} \mathbf{\Delta}_{\mathrm{j}} = \mathbf{U}_{\mathrm{j}}^\dagger\mathbf{M}_{\mathrm{j}}^{\mathrm{w}}\mathbf{U}_{\mathrm{j}} &= \frac{1}{\sqrt{2}}\sum_{k=1}^{2} v_k\mathbf{U}_{\mathrm{j}}^\dagger\mathbf{Y}_k^{\mathrm{w,j}}\mathbf{U}_{\mathrm{j}} = \frac{1}{\sqrt{2}}\sum_{k=1}^{2} v_k\tilde{\mathbf{Y}}_k^{\mathrm{j}}, \\ \mathrm{j} &= u, d, l, \nu_D, \end{aligned} \tag{28}$$

where $\tilde{\mathbf{Y}}_k^{\mathrm{j}} = \mathbf{U}_{\mathrm{j}}^\dagger\mathbf{Y}_k^{\mathrm{w,j}}\mathbf{U}_{\mathrm{j}}$ are the Yukawa matrices in the mass basis. Now, with the help of the orthogonal matrix given in Eq. (25) and the fact that the mass spectrum of Dirac particles only has the normal hierarchy, it is easy to obtain that the elements of the Yukawa matrices $\tilde{\mathbf{Y}}_k^{\mathrm{j}}$ can be expressed in terms of the geometric mean of the Dirac fermion masses normalized with respect to the electroweak scale, i.e.,

$$(\tilde{\mathbf{Y}}_k^{\mathrm{j}})_{\mathrm{rt}} = \frac{\sqrt{m_{\mathrm{j r}}m_{\mathrm{j t}}}}{v}(\tilde{\boldsymbol{\chi}}_k^{\mathrm{j}})_{\mathrm{rt}} \quad (\mathrm{r}, \mathrm{t} = 1, 2, 3). \tag{29}$$

Here, $(\tilde{\boldsymbol{\chi}}_k^{\mathrm{j}})_{\mathrm{rt}}$ are complex parameters, whose explicit forms are given in Appendix B. In the literature, this last relation is called the Cheng-Sher ansatz [45], which is associated with Higgs-fermion couplings. Also, the result obtained in Eq. (29) can be extended to any Hermitian mass matrix that may be brought to a two-zero-texture matrix by means of a unitary transformation.

As is known, the 2HDM-III is a generic description of particle physics at a higher energy scale ($\gtrsim$TeV), and its imprint at low energies is reflected in the Yukawa coupling structure. A detailed study of the Yukawa Lagrangian within the 2HDM-III was given in Refs. [23,24,40,46,47], while the phenomenological implications of this model in the scalar sector including lepton violation and/or FCNCs were presented in Refs. [48–50]. In those works, the FCNCs were under control because the authors assumed that the Yukawa matrices in the weak and mass bases are represented by means of a Hermitian matrix with two texture zeros and the Cheng-Sher ansatz, respectively. In our model ν2HDM $\otimes S_3$, the shape of the two texture zeros for the Yukawa matrices is obtained by imposing a flavor symmetry S_3 and from its explicit sequential breaking according to the chain $S_{3L}^{\mathrm{j}} \otimes S_{3R}^{\mathrm{j}} \supset S_3^{\mathrm{diag}} \supset S_2^{\mathrm{diag}}$. An immediate consequence of the above is that the Yukawa matrices in the mass basis naturally take the form of the so-called Cheng-Sher ansatz. Therefore, we can say that the FCNCs are under control in the ν2HDM $\otimes S_3$.

The lepton flavor-mixing matrix is defined as $\mathbf{U}_{\mathrm{PMNS}} = \mathbf{U}_l^\dagger\mathbf{U}_\nu$ [51]. In this context the Pontecorvo-Maki-Nakagawa-Sakata (PMNS) matrix takes the form

$$\mathbf{U}_{\mathrm{PMNS}} = \mathbf{O}_l^\top\mathbf{P}^{(\nu-l)}\mathbf{O}_\nu^{\mathrm{n[i]}}, \tag{30}$$

where $\mathbf{P}^{(\nu-l)} = \mathrm{diag}(1, e^{i\phi_{\ell 1}}, e^{i\phi_{\ell 2}})$ with $\phi_{\ell 1} = \phi_l - 2\phi_\nu$ and $\phi_{\ell 2} = \phi_l - \phi_\nu$. The explicit forms of the entries of the PMNS matrix are given in Appendix C. The first conclusion of this PMNS matrix is that the unitary matrix $\mathbf{U}_{\mathrm{s}}$—the one that allows us to pass from the weak basis to the flavor-symmetry-adapted basis—is unobservable in the lepton flavor-mixing matrix.

C. The mixing angle and *CP* violation phases

In the symmetric parametrization of the lepton flavor-mixing matrix, the relations between the mixing angles and the entries of the PMNS matrix are [51,52]

$$\begin{aligned} \sin^2\theta_{13} &\equiv |(\mathbf{U}_{\mathrm{PMNS}})_{13}|^2, \qquad \sin^2\theta_{12} \equiv \frac{|(\mathbf{U}_{\mathrm{PMNS}})_{12}|^2}{1-|(\mathbf{U}_{\mathrm{PMNS}})_{13}|^2}, \\ \sin^2\theta_{23} &\equiv \frac{|(\mathbf{U}_{\mathrm{PMNS}})_{23}|^2}{1-|(\mathbf{U}_{\mathrm{PMNS}})_{13}|^2}. \end{aligned} \tag{31}$$

On the one hand, the lepton Jarlskog invariant which appears in conventional neutrino oscillations is defined as

$$\mathcal{J}_{CP} = \mathcal{I}m\{(\mathbf{U}_{\mathrm{PMNS}})_{11}^*(\mathbf{U}_{\mathrm{PMNS}})_{23}^*(\mathbf{U}_{\mathrm{PMNS}})_{13}(\mathbf{U}_{\mathrm{PMNS}})_{21}\}, \tag{32}$$

and in the symmetric parametrization it has the form

$$\mathcal{J}_{CP} = \frac{1}{8}\sin 2\theta_{12}\sin 2\theta_{23}\sin 2\theta_{13}\cos\theta_{13}\sin\delta_{CP}, \tag{33}$$

where $\delta_{CP} = \phi_{13} - \phi_{23} - \phi_{12}$. Moreover, the invariants

$$\mathcal{I}_1 = \mathcal{I}m\{(\mathbf{U}_{\rm PMNS})^2_{12}(\mathbf{U}_{\rm PMNS})^{*2}_{11}\} \quad \text{and}$$
$$\mathcal{I}_2 = \mathcal{I}m\{(\mathbf{U}_{\rm PMNS})^2_{13}(\mathbf{U}_{\rm PMNS})^{*2}_{11}\} \tag{34}$$

associated with the Majorana phases [53–55] take the form

$$\mathcal{I}_1 = \frac{1}{4}\sin^2 2\theta_{12}\cos^4\theta_{13}\sin(-2\phi_{12}) \quad \text{and}$$
$$\mathcal{I}_2 = \frac{1}{4}\sin^2 2\theta_{13}\cos^2\theta_{12}\sin(-2\phi_{13}). \tag{35}$$

Then, the phase factors associated with the CP violation can be written as

$$\sin(\delta_{CP}) = \frac{\mathcal{J}_{\rm CP}(1-|(\mathbf{U}_{\rm PMNS})_{13}|^2)}{|(\mathbf{U}_{\rm PMNS})_{11}||(\mathbf{U}_{\rm PMNS})_{12}||(\mathbf{U}_{\rm PMNS})_{13}||(\mathbf{U}_{\rm PMNS})_{23}||(\mathbf{U}_{\rm PMNS})_{33}|},$$
$$\sin(-2\phi_{12}) = \frac{\mathcal{I}_1}{|(\mathbf{U}_{\rm PMNS})_{11}|^2|(\mathbf{U}_{\rm PMNS})_{12}|^2}, \qquad \sin(-2\phi_{13}) = \frac{\mathcal{I}_2}{|(\mathbf{U}_{\rm PMNS})_{11}|^2|(\mathbf{U}_{\rm PMNS})_{13}|^2}. \tag{36}$$

The equivalence between the Particle Data Group (PDG) and symmetric parameterization may be expressed as $\mathbf{U}_{\rm PDG} = \mathbf{K}\mathbf{U}_{\rm Sym}$, where $\mathbf{K} = {\rm diag}(1, e^{i\frac{\alpha_{21}}{2}}, e^{i\frac{\alpha_{31}}{2}})$ with $\delta_{CP} = \phi_{13} - \phi_{23} - \phi_{12}$, $\alpha_{21} = -2\phi_{12}$ and $\alpha_{31} = -2(\phi_{12} + \phi_{23})$.

III. NUMERICAL ANALYSIS

In the three-flavor neutrino scheme there are six independent parameters which determine the behavior of neutrino oscillation phenomena: the flavor-mixing angles, the "Dirac-like" CP-violating phase, and the squared-mass splitting. The latest neutrino oscillation parameter is defined as $\Delta m^2_{ij} \equiv m^2_{\nu_i} - m^2_{\nu_j}$, in agreement with the results obtained in the global fit reported in Ref. [20]. These neutrino oscillation parameters have the following numerical values [at the best-fit point (BFP) $\pm 1\sigma$ and 3σ][5]:

$$\Delta m^2_{21}(10^{-5}\ {\rm eV}^2) = 7.50^{+0.19}_{-0.17}, \quad 7.03 - 8.09,$$
$$\Delta m^2_{31}(10^{-3}\ {\rm eV}^2) = 2.524^{+0.039}_{-0.040}, \quad 2.407 - 2.643, \quad \text{for NH},$$
$$\Delta m^2_{23}(10^{-3}\ {\rm eV}^2) = 2.514^{+0.038}_{-0.041}, \quad 2.399 - 2.635, \quad \text{for IH}. \tag{37}$$

From the definition of the squared-mass splitting Δm^2_{ij}, two of neutrino masses can be written as

$$m_{\nu_{3[2]}} = \sqrt{m^2_{\nu_{1[3]}} + \Delta m^2_{31[23]}} \quad \text{and}$$
$$m_{\nu_{2[1]}} = \sqrt{m^2_{\nu_{1[3]}} + \Delta m^2_{21[31]}}, \tag{38}$$

where $m_{\nu_{1[3]}}$ is the lightest neutrino mass.[6] Also, this neutrino mass is considered as the only free parameter in the above expressions, since the mass-squared differences Δm^2_{ij} are determined by experiment.

From the results reported by the Planck Collaboration for cosmological parameters, the upper limit on the active neutrino mass sum is $\sum m_{\nu_i} < 0.23$ eV for an active neutrino number equal to $N_{eff} = 3.15 \pm 0.23$ [56]. This upper bound is independent of the hierarchy in the neutrino mass spectrum. So, with all of the above experimental information and considering the expressions in Eq. (38), we can obtain the following ranged for the neutrino masses:

$$m_{\nu_1}(10^{-2}\ {\rm eV}) = \begin{cases} [0.00, 7.10], \\ [4.90, 8.25], \end{cases}$$
$$m_{\nu_2}(10^{-2}\ {\rm eV}) = \begin{cases} [0.84, 7.13], \\ [4.97, 8.30], \end{cases}$$
$$m_{\nu_3}(10^{-2}\ {\rm eV}) = \begin{cases} [4.80, 8.75], \\ [0, 6.45]. \end{cases} \tag{39}$$

Here, the oscillation parameters Δm^2_{ij} are taken within the currently allowed 3σ range [20]. The values in the first and second rows correspond to a normal and inverted hierarchy in the neutrino mass spectrum, respectively. For both hierarchies there is the possibility that the lightest neutrino mass could be zero. Namely, in this case the lightest neutrino is a massless particle. In Fig. 1 we show the behavior of the neutrino masses (right panel) and the sum of neutrino masses (left panel) as functions of the lightest neutrino mass m_ν.

A. The likelihood test χ^2

To validate our hypothesis where the S_3 horizontal flavor symmetry is explicitly sequentially broken according to the chain $S^{\rm j}_{3L} \otimes S^{\rm j}_{3R} \supset S^{\rm diag}_3 \supset S^{\rm diag}_2$ (and hence all fermion mass matrices are represented through a matrix with two texture zeros), we make a likelihood test where the χ^2 function is defined as

[5]Here, NH and IH denote the normal and inverted hierarchy in the neutrino mass spectrum, respectively.

[6]The subscripts i and j denote the normal and inverted hierarchy in the neutrino mass spectrum.

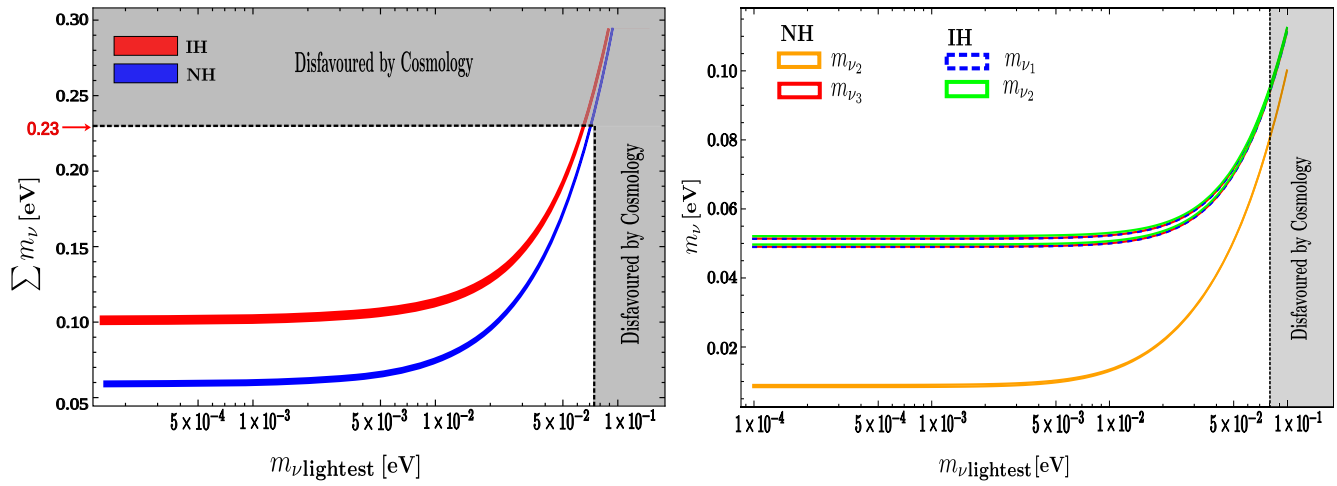

FIG. 1. In the left panel we show the sum of neutrino masses. The right panel shows the neutrino masses. The neutrino oscillation parameters Δm^2_{ij} are taken within the currently allowed 3σ range [20]. The upper bound on the mass of the lightest neutrino is obtained from the Planck result, where $\sum m_{\nu_i} < 0.23$ eV at the 95% level [56].

$$\chi^2 = \sum_{i<j}^{3} \frac{(\sin^2\theta_{ij}^{\text{exp}} - \sin^2\theta_{ij}^{\text{th}})^2}{\sigma^2_{\theta ij}}. \tag{40}$$

In this expression, the superscript "th" is used to denote the theoretical expressions of lepton mixing angles, while the terms with the superscript "exp" denote the experimental data with an uncertainty $\sigma_{\theta_{ij}}$ for lepton mixing angles. For the latter, we consider the following values, at BFP $\pm 1\sigma$ [20]:

$$\begin{aligned}
&\sin^2\theta_{12}^{\text{exp}}(10^{-1}) = 3.06 \pm 0.12,\\
&\sin^2\theta_{23}^{\text{exp}}(10^{-1}) = \begin{cases} 4.41^{+0.27}_{-0.21}, \\ 5.87^{+0.20}_{-0.24}, \end{cases}\\
&\sin^2\theta_{13}^{\text{exp}}(10^{-2}) = \begin{cases} 2.166 \pm 0.0075, \\ 2.179 \pm 0.0076. \end{cases}
\end{aligned} \tag{41}$$

The values in the first and second rows correspond to the normal and inverted hierarchy in the neutrino mass spectrum, respectively. From Eqs. (25), (30), (31), and (38), it is easy to conclude that the χ^2 function depends on five free parameters: $\chi^2 = \chi^2(\Phi_{\ell 1}, \Phi_{\ell 2}, \delta_\ell, \delta_\nu, m_{\nu_{1[3]}})$. However, the χ^2 function depends only on three experimental values which correspond to the leptonic flavor-mixing angles. Therefore, if we simultaneously consider $\Phi_{\ell 1}$, $\Phi_{\ell 2}$, δ_ℓ, δ_ν, and $m_{\nu_{1[3]}}$ as free parameters in the likelihood test, we can only determine the values of these parameters at the BFP. In accordance with the above, we first seek the BFP by means of a likelihood test where the χ^2 function have all five free parameters: $\Phi_{\ell 1}$, $\Phi_{\ell 2}$, δ_ℓ, δ_ν, and $m_{\nu_{1[3]}}$. To minimize the χ^2 function, we have scanned the parameter space by considering the following values for the charged lepton masses [34]:

$$\begin{aligned}
m_e &= 0.5109998928 \pm 0.000000011,\\
m_\mu &= 105.6583715 \pm 0.0000035,\\
m_\tau &= 1776.82 \pm 0.16.
\end{aligned} \tag{42}$$

The experimental values for the leptonic mixing angles are given in Eq. (41).

In Table I we show the numerical values obtained at the BFP for the five parameters, the lepton mixing angles, and

TABLE I. Numerical values obtained at the BFP for the five parameters, the lepton mixing angles, and the phase factors associated with the CPV. These results were obtained by considering Δm^2_{ij} at the BFP and in the ranges BFP $\pm\,\sigma$ and 3σ [20], and simultaneously $\Phi_{\ell 1}$, $\Phi_{\ell 2}$, δ_ℓ, δ_ν, and $m_{\nu_{1[3]}}$ are free parameters in the χ^2 function.

	Δm^2_{ij} at	$\Phi_{\ell 1}[^\circ]$	$\Phi_{\ell 2}[^\circ]$	$m_{\nu_{\text{lightest}}}$ [eV]	δ_ℓ	δ_ν	$\theta_{12}^{\text{th}}[^\circ]$	$\theta_{23}^{\text{th}}[^\circ]$	$\theta_{13}^{\text{th}}[^\circ]$	$\delta_{\text{CP}}[^\circ]$	$\phi_{12}[^\circ]$	$\phi_{13}[^\circ]$	χ^2_{min}
NH	3σ	270	195	2.57×10^{-3}	0.20460	0.63519	33.58	41.60	8.47	−68.65	−5.86	14.77	4.63×10^{-4}
	BFP $\pm 1\sigma$	270	195	2.57×10^{-3}	0.22256	0.64507	33.59	41.61	8.46	−70.74	−5.79	14.67	3.13×10^{-4}
	BFP	270	195	2.57×10^{-3}	0.21492	0.64008	33.80	41.63	8.45	−69.85	−5.80	14.73	8.75×10^{-2}
IH	3σ	290	187	2.49×10^{-2}	0.59943	0.01999	33.67	50.08	8.48	−80.90	−5.25	−2.18	2.30×10^{-2}
	BFP $\pm 1\sigma$	290	187	2.49×10^{-2}	0.59888	0.01995	33.74	50.05	8.49	−80.88	−5.25	−2.18	4.56×10^{-2}
	BFP	290	187	2.49×10^{-2}	0.59798	0.01971	33.83	49.99	8.49	−80.83	−5.25	−2.19	1.08×10^{-1}

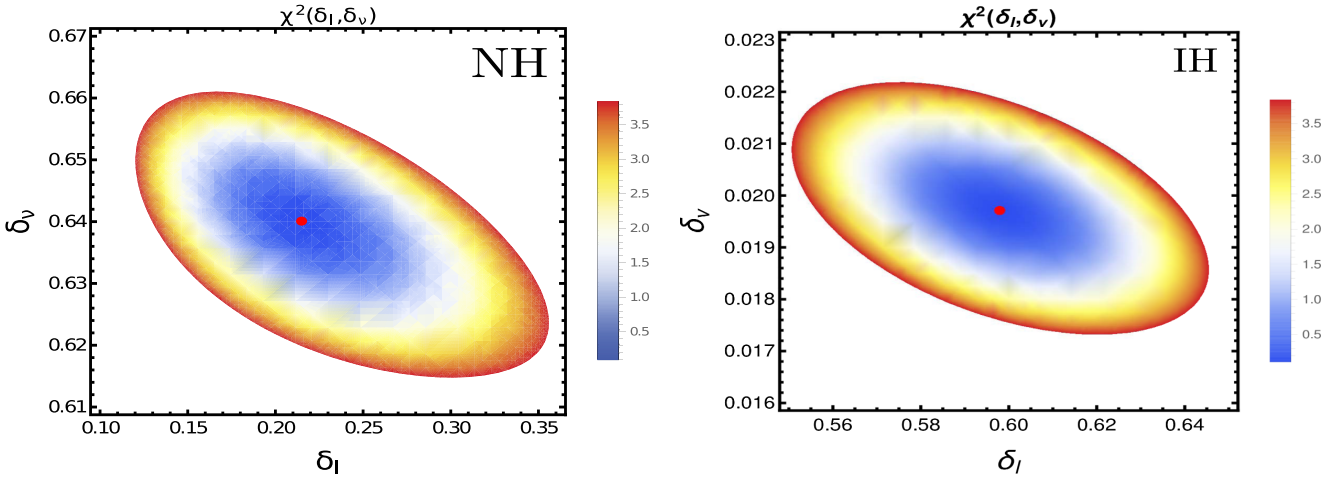

FIG. 2. The allowed regions in the parameter space for δ_l and δ_ν at 3σ C.L.; the red point (•) represents the BFP. The left panel is for the normal hierarchy, while the right panel is for the inverted hierarchy. Here, the parameters $m_{\nu_{1[3]}}$, ϕ_{l1}, and ϕ_{l2} are fixed to the values obtained when the Δm^2_{ij} neutrino oscillation parameters are given at the BFP; see Table I.

the phase factors associated with the CPV. All of these results were obtained by considering Δm^2_{ij} at the BFP and in the BFP $\pm\,\sigma$ and 3σ ranges, and simultaneously $\Phi_{\ell 1}$, $\Phi_{\ell 2}$, δ_ℓ, δ_ν, and $m_{\nu_{1[3]}}$ are free parameters in the χ^2 function of the likelihood test.

Now, as we know the numerical values of the five free parameters at the BFP, we perform a new χ^2 analysis for the case when the oscillation parameters Δm^2_{ij} take the values at the BFP and where we fix $m_{\nu_{1[3]}}$, $\Phi_{\ell 1}$, and $\Phi_{\ell 2}$ to the values given in Table I.

So, the $\chi^2 = \chi^2(\delta_l, \delta_\nu)$ function implies one degree of freedom. In Fig. 2, we show the allowed regions in the parameter space for δ_l and δ_ν at 3σ C.L., where a red point (•) represents the BFP. The left panel is for the normal hierarchy, and we can see that δ_ν and δ_l are of the order of 10^{-1}. The right panel is for the inverted hierarchy, and here δ_ν is $\sim 10^{-1}$, while δ_l is of the order of 10^{-2}.

Associated to the parameter regions of δ_ν and δ_l given in Fig. 2 for both hierarchies in the neutrino mass spectrum, and based on Eq. (36), we find the regions predicted by the ν2HDM $\otimes$ S_3 for a "Dirac-like" phase δ_{CP}. These regions are shown in Fig. 3. In concordance with experimental data, the plots of mixing angles versus δ_l are more restricted than those versus δ_ν. These results correspond closely with allowed regions obtained in the global fit reported in Ref. [20].

In the same way, we analyze the three leptonic flavor-mixing angles for both hierarchies, but in Fig. 4 we just show the allowed regions for the atmospheric mixing angle θ_{23} at the BFP, $\pm 1\sigma$, and 3σ C.L. In order to round the above results, from our analysis we obtain the following values for the three mixing angles at BFP $\pm\, 1\sigma$ C.L.:

$$\sin^2\theta_{12}^{\rm th}(10^{-1}) = \begin{cases} 3.09^{+0.066}_{-0.065}, \\ 3.10^{+0.011}_{-0.011}, \end{cases}$$
$$\sin^2\theta_{23}^{\rm th}(10^{-1}) = \begin{cases} 4.41^{+0.10}_{-0.14}, \\ 5.87^{+0.224}_{-0.223}, \end{cases}$$
$$\sin^2\theta_{13}^{\rm th}(10^{-2}) = \begin{cases} 2.160 \pm 0.14, \\ 2.177 \pm 0.12. \end{cases} \qquad (43)$$

We also obtain the following allowed value ranges at BFP $\pm\, 1\sigma$ for the "Dirac-like" phase $\delta_{\rm CP}$, as well as for the two Majorana phase factors ϕ_{12} and ϕ_{13}:

$$\delta_{CP}(^\circ) = \begin{cases} -69.8^{+5.508}_{-6.110}, \\ -80.83^{+0.652}_{-0.709}, \end{cases} \qquad \phi_{12}(^\circ) = \begin{cases} -5.800^{+0.170}_{-0.150}, \\ -5.24^{+0.153}_{-0.148}, \end{cases}$$
$$\phi_{13}(^\circ) = \begin{cases} 14.744^{+1.266}_{-1.366}, \\ -2.190^{+0.0030}_{-0.0005}. \end{cases} \qquad (44)$$

From Eq. (44) and Table I we can conclude that values for the phase $\delta_{\rm CP}$ obtained in our scheme are consistent with a maximal *CP* violation.

Finally, as an immediate result of the above likelihood analysis, the magnitude of the entries of the $\mathbf{U}_{\rm PMNS}$ mixing matrix can be computed numerically. So, at 3σ C.L., the $\mathbf{U}_{\rm PMNS}$ matrix takes the form

$$\begin{pmatrix} 0.822^{+0.0044}_{-0.0045} & 0.550^{+0.0055}_{-0.0054} & 0.147^{+0.0047}_{-0.0048} \\ 0.395^{+0.0181}_{-0.0154} & 0.642^{+0.0008}_{-0.0001} & 0.657^{+0.0082}_{-0.0111} \\ 0.410^{+0.0056}_{-0.0089} & 0.534^{+0.0045}_{-0.0056} & 0.739^{+0.0088}_{-0.0064} \end{pmatrix}$$
(normal hierarchy), (45)

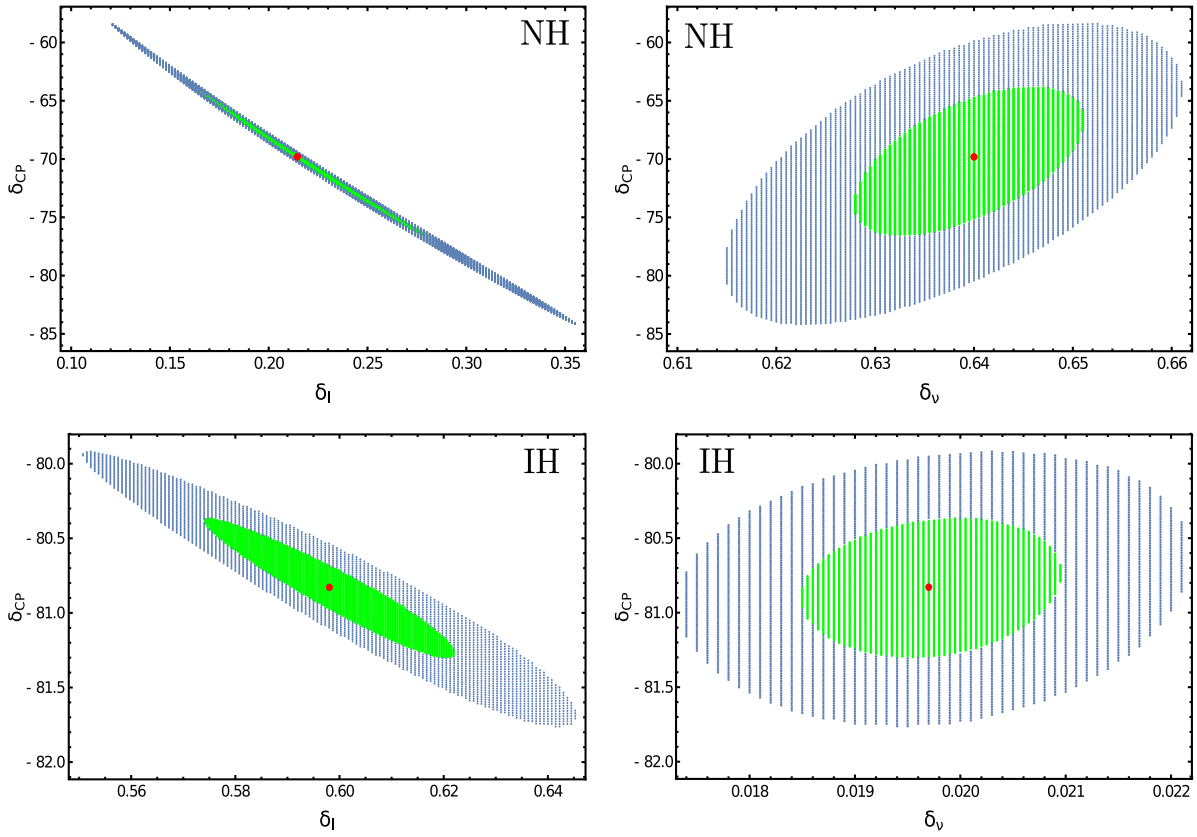

FIG. 3. The allowed regions for a "Dirac-like" CPV phase $\delta_{\rm CP}$, and the free parameters δ_l and δ_ν. The parameters $m_{\nu_{1[3]}}$, $\Phi_{\ell 1}$ and $\Phi_{\ell 2}$ are fixed to the values given in Table I for the BFP. The BFP is denoted by a red point •, and the green and blue regions are for 1σ and 3σ C.L., respectively. The upper and lower panels correspond to the normal and inverted hierarchy, respectively.

$$\begin{pmatrix} 0.822^{+0.0012}_{-0.0012} & 0.551^{+0.0007}_{-0.0006} & 0.147^{+0.0041}_{-0.0041} \\ 0.355^{+0.0072}_{-0.0071} & 0.547^{+0.0144}_{-0.0149} & 0.758^{+0.0138}_{-0.0141} \\ 0.446^{+0.0077}_{-0.0080} & 0.630^{+0.0120}_{-0.0122} & 0.636^{+0.0174}_{-0.0178} \end{pmatrix} \quad \text{(inverted hierarchy)}. \tag{46}$$

IV. PHENOMENOLOGICAL IMPLICATIONS

In the previous section we have seen that in our theoretical framework, where the S_3 flavor symmetry implies that the fermion mass matrices should have two texture zeros, we can reproduce values of the oscillation parameters that are in very good agreement with the latest experimental data. In the following, we shall investigate the phenomenological implications of these results for neutrinoless double-beta decay ($0\nu\beta\beta$) and CP violation in neutrino oscillations in matter.

A. Neutrinoless double-beta decay

The decay $0\nu\beta\beta$ is a rare second-order weak process where a nucleus (A, Z) decays into another one by the emission of two electrons, whose decay mode is $(A, Z) \to (A, Z+2) + e^- + e^-$. The observation of this process would establish that neutrinos are Majorana particles and that total lepton number is not a conserved symmetry in nature [57,58]. In the most simple version of this process, the amplitude for the decay is proportional to a quantity called the effective mass m_{ee} [59–61]. In the symmetric parametrization of the lepton mixing matrix the effective mass parameter has the form [62,63]

$$|m_{ee}| = |m_{\nu_1}\cos^2\theta_{12}\cos^2\theta_{13} + m_{\nu_2}\sin^2\theta_{12}\cos^2\theta_{13}e^{-i2\phi_{12}} + m_{\nu_3}\sin^2\theta_{13}e^{-i2\phi_{13}}|, \tag{47}$$

where ϕ_{12} and ϕ_{13} are the Majorana phases given in Eq. (36). In Fig. 5 we show the allowed regions for the magnitude of the effective mass parameter m_{ee}, which were obtained in the context of ν2HDM $\otimes$ S_3. Each of these regions was obtained by setting the values of some of the five free parameters in the χ^2 function (40) to the values given in Table I for Δm^2_{ij} at the BFP. Then, for both hierarchies in the lower panels of Fig. 5, the blue lines were

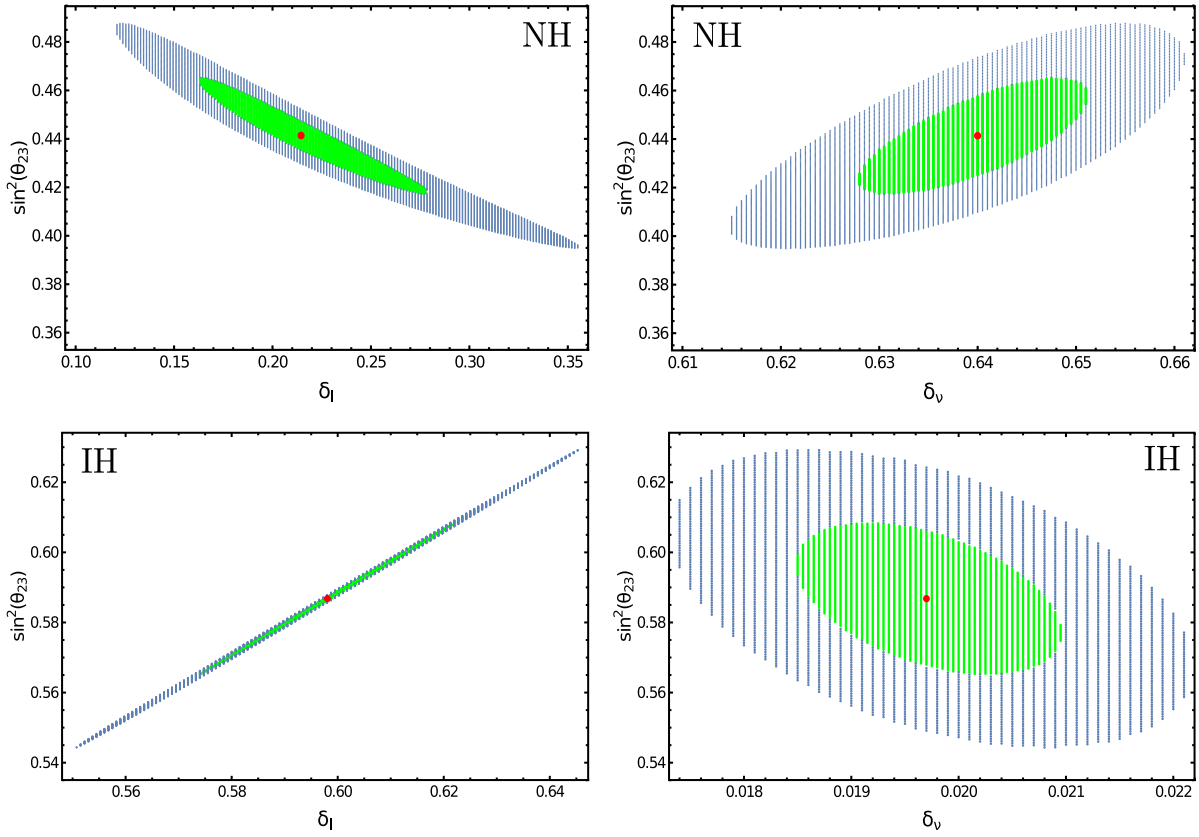

FIG. 4. The allowed regions for the atmospheric mixing angle $\sin^2\theta_{23}$ and the free parameters δ_l and δ_ν. The parameters $m_{\nu_{1[3]}}$, $\Phi_{\ell 1}$, and $\Phi_{\ell 2}$ are fixed to the values given in Table I, when the oscillation parameters Δm^2_{ij} take the values at the BFP. The BFP is denoted by a red point •, and the green and blue regions are for 1σ and 3σ C.L., respectively. The upper and lower panels correspond to the normal and inverted hierarchy, respectively.

obtained by a likelihood test where the values of $\phi_{\ell 1}$, $\phi_{\ell 2}$, δ_e, and δ_ν are fixed, while $m_{\nu_{\text{lightest}}}$ is a free parameter. The orange bands were obtained by a likelihood test where the values of $\phi_{\ell 2}$, δ_e, and δ_ν are fixed, while $m_{\nu_{\text{lightest}}}$ and $\phi_{\ell 1}$ are free parameters. The yellow bands were obtained by a likelihood test where the values of $\phi_{\ell 1}$, δ_e, and δ_ν are fixed, while $m_{\nu_{\text{lightest}}}$ and $\phi_{\ell 2}$ are free parameters. The sky blue bands were obtained by a likelihood test where the values of $\phi_{\ell 1}$, $\phi_{\ell 2}$, and δ_ν are fixed, while $m_{\nu_{\text{lightest}}}$ and δ_e are free parameters. Finally, the turquoise bands were obtained by a likelihood test where the values of $\phi_{\ell 1}$, $\phi_{\ell 2}$, and δ_e are fixed, while $m_{\nu_{\text{lightest}}}$ and δ_ν are free parameters.

To round. the previous results, in Table II we show the allowed numerical ranges at 95% C.L. for the magnitude of the effective mass parameter m_{ee} and the lightest neutrino mass $m_{\nu_{\text{lightest}}}$. From the results in Table II it is easy to conclude that for the normal hierarchy $m_{\nu_1} \sim 2\times 10^{-3}$ eV and $|m_{ee}| \sim 3\times 10^{-3}$ eV, while for the inverted hierarchy $m_{\nu_3} \sim 2\times 10^{-2}$ eV and $|m_{ee}| \sim 3\times 10^{-2}$ eV.

B. *CP* violation in neutrino oscillations in matter

In recent years, we have entered a precision era in the determination of flavor leptonic mixing angles. However, it is not the same situation for *CP* violation in this sector, since the numerical value of the *CP* violation phase has yet to be experimentally determined. But we have a hunch about where to look: the neutrino oscillations with matter effects [67]. One of the aims of the LBL neutrino experiments such as T2K [68] and NOνA [69], as well as the proposed experiment DUNE [70], is determination of the "Dirac-like" *CP* violation phase and other parameters that rule the neutrino oscillations $\nu_\mu \to \nu_e$ and $\bar{\nu}_\mu \to \bar{\nu}_e$. The transition probabilities in matter for the oscillation between electron and muon neutrinos and between electron and muon antineutrinos have the form [63,71,72]

$$P(\nu_\mu \to \nu_e) \simeq P_{\text{atm}} + P_{\text{sol}} + 2\sqrt{P_{\text{atm}}}\sqrt{P_{\text{sol}}}\cos(\Delta_{32} + \delta_{\text{CP}}),$$
$$P(\bar{\nu}_\mu \to \bar{\nu}_e) \simeq \mathcal{P}_{\text{atm}} + P_{\text{sol}} + 2\sqrt{\mathcal{P}_{\text{atm}}}\sqrt{P_{\text{sol}}}\cos(\Delta_{32} - \delta_{\text{CP}}), \tag{48}$$

where

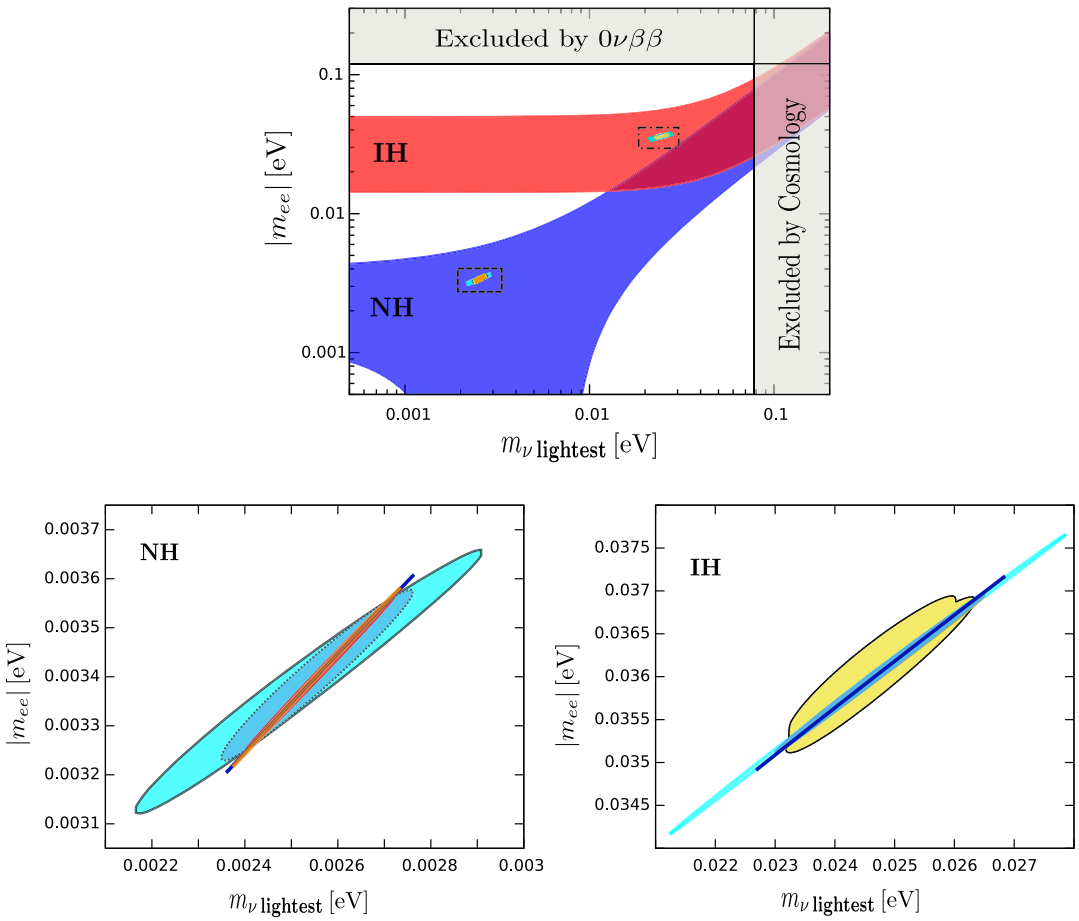

FIG. 5. In the upper panel we show the effective mass $|m_{ee}|$ which is involved in the $0\nu\beta\beta$ decay. The red and blue bands are obtained with the current experimental data on neutrino oscillations, at 3σ [20], for an inverted and normal neutrino mass hierarchy, respectively. On the one hand, from the combination of EXO-200 [64,65] and KamLAND-ZEN [66] results the upper bound is $|m_{ee}| < 0.120$ eV. On the other hand, from the results reported by the Planck Collaboration we have that $\sum_i m_i < 0.230$ eV at the 95% level [56]; thus, an upper bound on the lightest neutrino mass is established. In the bottom-left and -right lower panels we show a zoom in of the allowed regions for $|m_{ee}|$ obtained at 95% C.L. in the context of ν2HDM $\otimes$ S_3 for a normal and inverted hierarchy, respectively.

TABLE II. The allowed numerical ranges at 95% C.L. for the effective mass parameter magnitude m_{ee} and the lightest neutrino mass $m_{\nu_{\text{lightest}}}$.

	Fixed parameters	$m_{\nu_{\text{lightest}}}[10^{-2}$ eV]	$\lvert m_{ee}\rvert[10^{-2}$ eV]
NH	$\phi_{\ell 1}$, $\phi_{\ell 2}$, δ_e, δ_ν	[0.2360, 0.2768]	[0.3204, 0.3608]
	$\phi_{\ell 2}$, δ_e, δ_ν	[0.2374, 0.2735]	[0.3215, 0.3583]
	$\phi_{\ell 1}$, δ_e, δ_ν	[0.2404, 0.2711]	[0.3251, 0.3563]
	$\phi_{\ell 1}$, $\phi_{\ell 2}$, δ_ν	[0.2349, 0.2761]	[0.3229, 0.3577]
	$\phi_{\ell 1}$, $\phi_{\ell 2}$, δ_e	[0.2164, 0.2908]	[0.3121, 0.3659]
IH	$\phi_{\ell 1}$, $\phi_{\ell 2}$, δ_e, δ_ν	[2.268, 2.685]	[3.491, 3.717]
	$\phi_{\ell 2}$, δ_e, δ_ν	[2.317, 2.635]	[3.511, 3.694]
	$\phi_{\ell 1}$, δ_e, δ_ν	[2.311, 2.650]	[3.515, 3.696]
	$\phi_{\ell 1}$, $\phi_{\ell 2}$, δ_ν	[2.301, 2.648]	[3.512, 3.695]
	$\phi_{\ell 1}$, $\phi_{\ell 2}$, δ_e	[2.123, 2.787]	[3.416, 3.767]

$$\sqrt{P_{\text{sol}}} = \cos\theta_{23}\sin 2\theta_{12}\frac{\sin aL}{aL}\Delta_{21},$$
$$\sqrt{P_{\text{atm}}} = \sin\theta_{23}\sin 2\theta_{13}\frac{\sin(\Delta_{31}-aL)}{(\Delta_{31}-aL)}\Delta_{31},$$
$$\sqrt{\mathcal{P}_{\text{atm}}} = \sin\theta_{23}\sin 2\theta_{13}\frac{\sin(\Delta_{31}+aL)}{(\Delta_{31}+aL)}\Delta_{31}. \tag{49}$$

In the above expressions, L is the baseline,

$$\Delta_{ij} = \frac{\Delta m^2_{ij}L}{4E}, \qquad \Delta m^2_{ij} = m^2_i - m^2_j \quad \text{and} \quad a = \frac{G_F N_e}{\sqrt{2}}. \tag{50}$$

Here, E is the energy of the neutrino beam, G_F is the Fermi constant, and N_e is the density of electrons. The parameter a is $a \approx (3500\ \text{km})^{-1}$ for the Earth's crust [71]. The asymmetry between $P(\nu_\mu \to \nu_e)$ and $P(\bar{\nu}_\mu \to \bar{\nu}_e)$ in matter is [72]

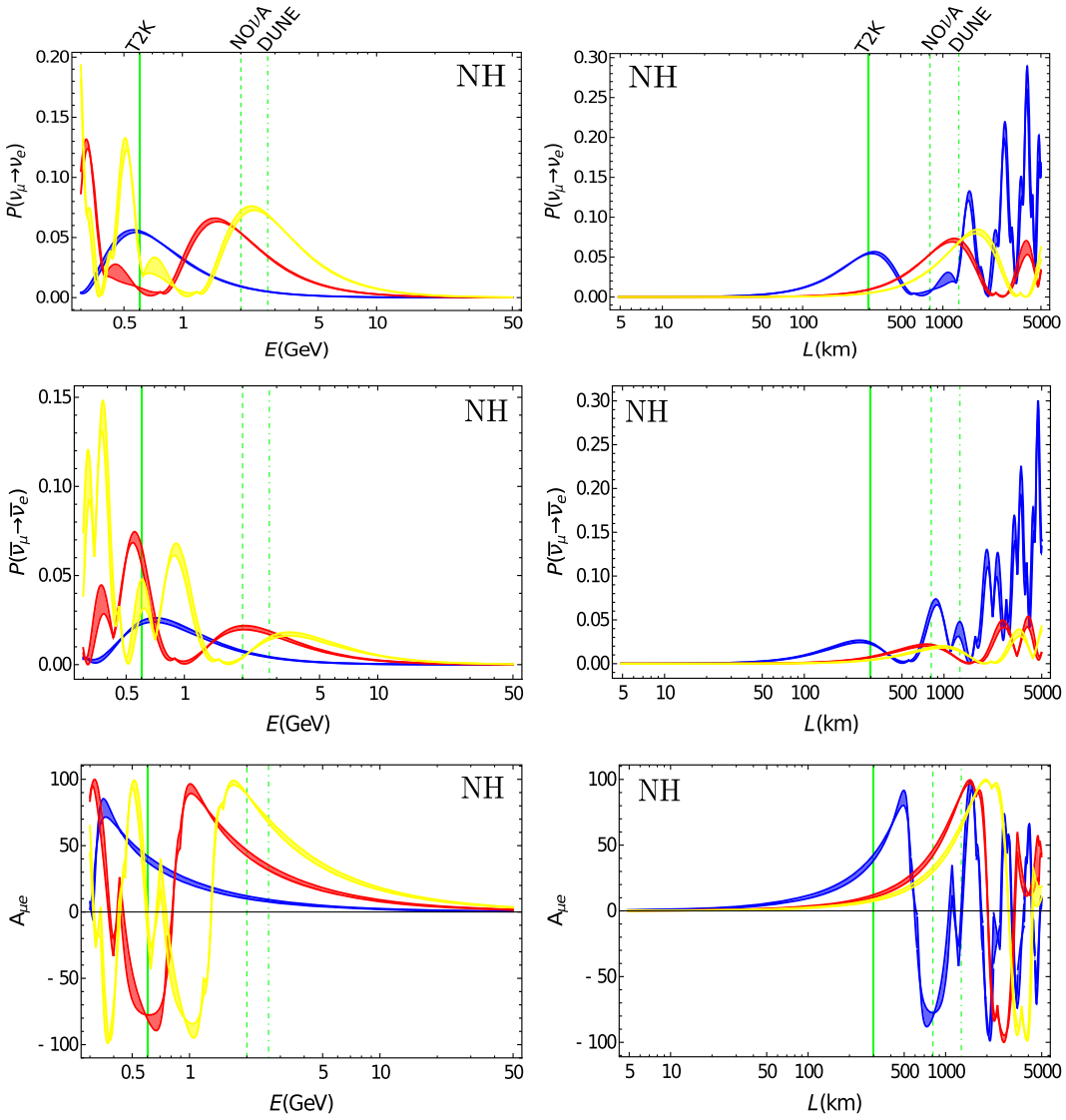

FIG. 6. The $P(\nu_\mu \to \nu_e)$ and $P(\bar{\nu}_\mu \to \bar{\nu}_e)$ transition probabilities, and the asymmetry $A_{\mu e}$ between them, for a normal hierarchy in the neutrino mass spectrum. The blue, red, and yellow bands are obtained for a baseline L of 295, 810, and 1300 km in the left panels. For the right panels these bands belong to a neutrino energy E of 0.3, 2, and 2.8 GeV, which correspond to the T2K, NOνA, and DUNE experiments, respectively. Here, the $\delta_{\rm CP}$ phase takes values within the 1σ C.L. range given in Eq. (44). The remaining parameters are fixed to the values obtained at the BFP, which are given in Eq. (37) for Δm^2_{ij} and Table I for flavor-mixing angles.

$$\mathcal{A}_{\mu e} = \frac{P(\nu_\mu \to \nu_e) - P(\bar{\nu}_\mu \to \bar{\nu}_e)}{P(\nu_\mu \to \nu_e) + P(\bar{\mu}_\nu \to \bar{\nu}_e)} = \frac{(P_{\rm atm} - \mathcal{P}_{\rm atm}) + 2\sqrt{P_{\rm sol}}(\sqrt{P_{\rm atm}}\cos(\Delta_{32} + \delta_{\rm CP}) - \sqrt{\mathcal{P}_{\rm atm}}\cos(\Delta_{32} - \delta_{\rm CP}))}{(P_{\rm atm} + \mathcal{P}_{\rm atm}) + 2\sqrt{P_{\rm sol}}(\sqrt{P_{\rm atm}}\cos(\Delta_{32} + \delta_{\rm CP}) + \sqrt{\mathcal{P}_{\rm atm}}\cos(\Delta_{32} - \delta_{\rm CP})) + 2P_{\rm sol}} \tag{51}$$

The above asymmetry $\mathcal{A}_{\mu e}$ is basically due to the absence of positrons in the journey of a neutrino (antineutrino) through the Earth. Hence, a neutrino experiment with a LBL would be more sensitive to this asymmetry.

The T2K neutrino oscillation experiment has a LBL of 295 km, while the energy of its neutrino beam has a peak around 0.6 GeV and a width of ~0.3 GeV [68]. In Figs. 6 and 7 (for normal and inverted hierarchies respectively), we show the transition probability

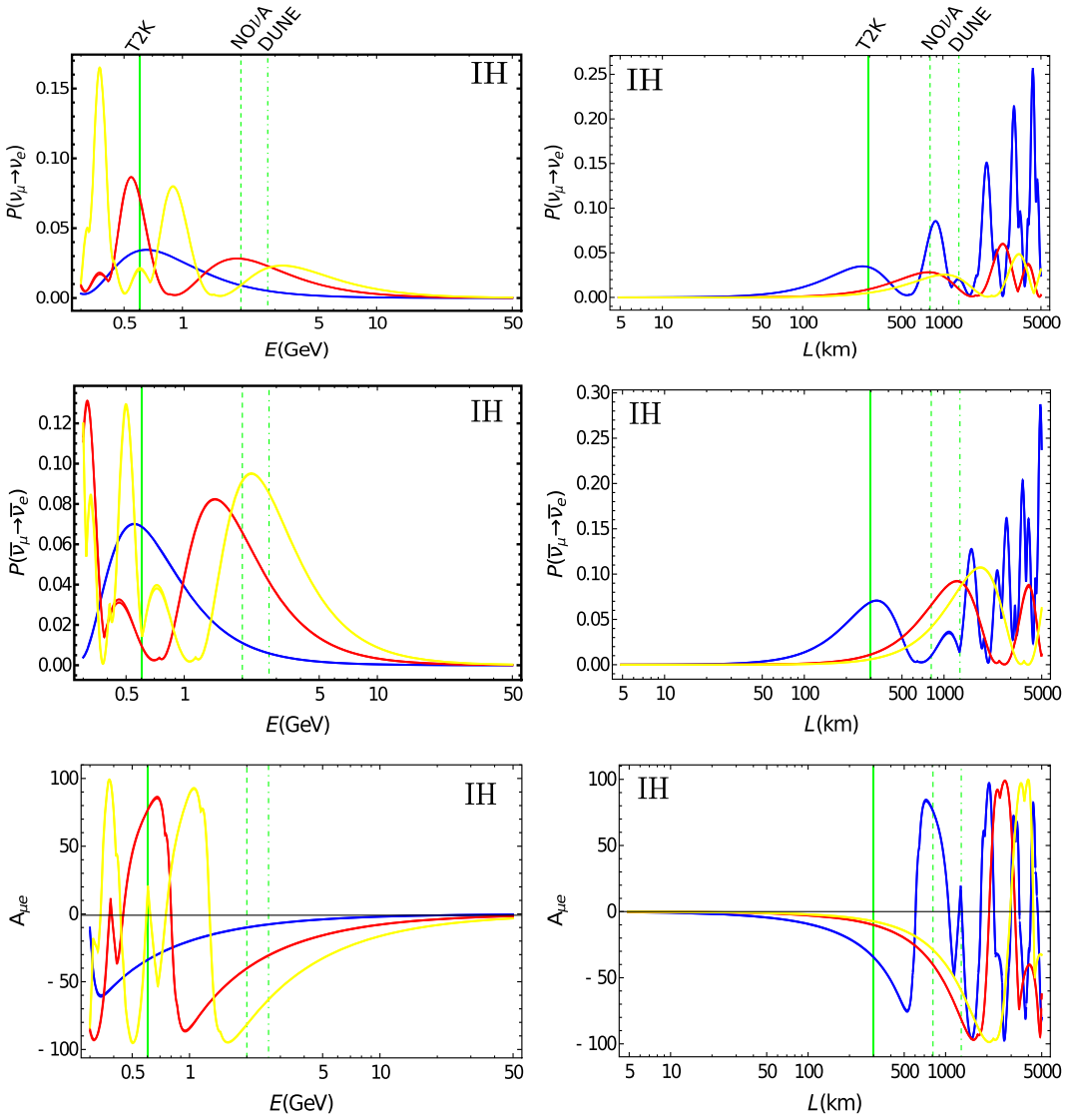

FIG. 7. The $P(\nu_\mu \to \nu_e)$ and $P(\bar{\nu}_\mu \to \bar{\nu}_e)$ transition probabilities and the asymmetry $A_{\mu e}$ between them for an inverted hierarchy in the neutrino mass spectrum. The blue, red, and yellow bands are obtained for a baseline L of 295, 810, and 1300 km in the left panels. For the right panels these bands belong to a neutrino energy E of 0.3, 2, and 2.8 GeV, which correspond to the T2K, NOνA, and DUNE experiments, respectively. Here, the $\delta_{\rm CP}$ phase takes values within the 1σ C.L. range given in Eq. (44). The remaining parameters are fixed to the values obtained at the BFP, which are given in Eq. (37) for Δm^2_{ij} and Table I for flavor-mixing angles.

$\nu_\mu(\bar{\nu}_\mu) \to \nu_e(\bar{\nu}_e)$ and the asymmetry $\mathcal{A}_{\mu e}$ for the T2K experiment.

The NOνA neutrino oscillation experiment has a LBL of 810 km, while the energy of its neutrino beam has a peak around 2 GeV [69]. In Figs. 6 and 7, we show the transition probability $\nu_\mu(\bar{\nu}_\mu) \to \nu_e(\bar{\nu}_e)$ and the asymmetry $\mathcal{A}_{\mu e}$ for the NOνA experiment.

Finally, the future neutrino oscillation experiment DUNE will have a LBL of ∼1300 km, while the energy of its neutrino beam will have a peak around 2.5–3.0 GeV [70]. In Figs. 6 and 7, the transition probability $\nu_\mu(\bar{\nu}_\mu) \to \nu_e(\bar{\nu}_e)$ and the asymmetry $\mathcal{A}_{\mu e}$ for the DUNE experiment are shown.

V. CONCLUSIONS

We have studied the theory of neutrino masses, mixings, and CPV as the realization of an S_3 flavor symmetry in the framework of the type-III two-Higgs-doublet model. In this ν2HDM $\otimes$ S_3 extension of the Standard Model, on the one hand, the active neutrinos acquire their small masses via the type-I seesaw mechanism. On the other hand, the explicit sequential breaking of flavor symmetry according to the chain $S^{\rm j}_{3L} \otimes S^{\rm j}_{3R} \supset S^{\rm diag}_3 \supset S^{\rm diag}_2$ allowed us to represent the Yukawa matrices in the flavor basis with a Hermitian matrix with two texture zeros. Consequently, we obtained a unified treatment for all fermion mass matrices in the

model, which are represented by a matrix with two texture zeros.

The unitary matrices that diagonalize the mass matrices were expressed in terms of fermion mass ratios. Then, the entries of the Yukawa matrices in the mass basis naturally acquired the form of the so-called Cheng-Sher ansatz. Also, the lepton flavor-mixing PMNS matrix was expressed as a function of the masses of charged leptons and neutrinos, two phases associated with CP violation, and two parameters associated with the flavor symmetry breaking. The unitary matrix that allows us to pass from the weak basis to the flavor-symmetry-adapted basis is unobservable in the Higgs-fermion couplings and lepton flavor mixing matrix.

To validate our hypothesis where the S_3 horizontal flavor symmetry is explicitly broken according to the chain $S_{3L}^{j} \otimes S_{3R}^{j} \supset S_3^{\mathrm{diag}} \supset S_2^{\mathrm{diag}}$, all fermion mass matrices were represented through a matrix with two texture zeros. Furthermore, we performed a likelihood test where we compared the theoretical expressions of the flavor-mixing angles with the current experimental data on the masses and flavor mixing of leptons. The results obtained in this χ^2 analysis are in very good agreement with the current experimental data.

We also obtained the following allowed value ranges, at BFP $\pm 1\sigma$, for the "Dirac-like" phase factor, as well as for the two Majorana phase factors:

$$\delta_{CP}(^\circ) = \begin{cases} -69.8^{+5.508}_{-6.110}, \\ -80.83^{+0.652}_{-0.709}, \end{cases} \qquad \phi_{12}(^\circ) = \begin{cases} -5.800^{+0.170}_{-0.150}, \\ -5.24^{+0.153}_{-0.148}, \end{cases}$$
$$\phi_{13}(^\circ) = \begin{cases} 14.744^{+1.266}_{-1.366}, \\ -2.190^{+0.0030}_{-0.0005}. \end{cases} \tag{52}$$

The upper (lower) row corresponds to the normal (inverted) hierarchy in the neutrino mass spectrum. These values of the phase factors are in agreement with a maximum CPV in neutrino oscillations in matter. Finally, we also analyzed the phenomenological implications of the above numerical values of the CP-violation phases on neutrinoless double-beta decay, as well as for LBL neutrino oscillation experiments such as T2K, NOνA, and DUNE.

ACKNOWLEDGMENTS

This work has been partially supported by Consejo Nacional de Ciencia y Tecnología (Conacyt) and Sistema Nacional de Investigadores (SNI), México. The authors thankfully acknowledge the computer resources, technical expertise, and support provided by the Laboratorio Nacional de Supercómputo del Sureste de México Conacyt network of national laboratories. F. G. C. acknowledges the financial support from Conacyt and Secretaría de Educación Pública-Programa para el Desarrollo Profesional Docente, para el Tipo Superior (SEP-PRODEP) under Grant No. 511-6/17-8017.

APPENDIX A: THREE-DIMENSIONAL REPRESENTATION OF S_3

The permutations of the symmetry group S_3 can be represented on the reducible triplet as [32,33]

$$\mathbf{D}^{(3)}(E) = \begin{pmatrix} 1 & 0 & 0 \\ 0 & 1 & 0 \\ 0 & 0 & 1 \end{pmatrix}, \quad \mathbf{D}^{(3)}(A_1) = \begin{pmatrix} 0 & 1 & 0 \\ 1 & 0 & 0 \\ 0 & 0 & 1 \end{pmatrix},$$
$$\mathbf{D}^{(3)}(A_2) = \begin{pmatrix} 0 & 0 & 1 \\ 1 & 0 & 0 \\ 0 & 1 & 0 \end{pmatrix}, \quad \mathbf{D}^{(3)}(A_3) = \begin{pmatrix} 1 & 0 & 0 \\ 0 & 0 & 1 \\ 0 & 1 & 0 \end{pmatrix},$$
$$\mathbf{D}^{(3)}(A_4) = \begin{pmatrix} 0 & 0 & 1 \\ 1 & 0 & 0 \\ 0 & 1 & 0 \end{pmatrix}, \quad \mathbf{D}^{(3)}(A_5) = \begin{pmatrix} 0 & 1 & 0 \\ 0 & 0 & 1 \\ 1 & 0 & 0 \end{pmatrix}. \tag{A1}$$

In this representation the projection operators take the form

$$\text{Symmetric singlet,} \quad \mathbf{P_1} = \frac{1}{3}\begin{pmatrix} 1 & 1 & 1 \\ 1 & 1 & 1 \\ 1 & 1 & 1 \end{pmatrix} = |v_{\mathbf{1}}\rangle\langle v_{\mathbf{1}}|,$$
$$\text{Antisymmetric singlet,} \quad \mathbf{P_{1'}} = 0,$$
$$\text{Doublet,} \quad \mathbf{P_2} = \frac{1}{3}\begin{pmatrix} 2 & -1 & -1 \\ -1 & 2 & -1 \\ -1 & -1 & 2 \end{pmatrix} = |v_{\mathbf{2A}}\rangle\langle v_{\mathbf{2A}}| + |v_{\mathbf{2S}}\rangle\langle v_{\mathbf{2S}}|, \tag{A2}$$

Here, the vector $|v_{\mathbf{1}}\rangle = \frac{1}{\sqrt{3}}(1,1,1)^\top$ is associated with the symmetric singlet. In the projection operator $\mathbf{P_2}$, we have the vectors $|v_{\mathbf{2A}}\rangle = \frac{1}{\sqrt{2}}(-1,1,0)^\top$ and $|v_{\mathbf{2S}}\rangle = \frac{1}{\sqrt{2}}(1,1,-2)^\top$, which are associated with the doublet.

Correspondingly, the vectors $|v_{\mathbf{2A}}\rangle$ and $|v_{\mathbf{2S}}\rangle$ are antisymmetric and symmetric, under the permutation of the first two elements. With the previous three vectors we can construct some tensors that can be helpful. Then,

$$|v_{\mathbf{2S}}\rangle\langle v_{\mathbf{2A}}| = \frac{1}{\sqrt{12}}\begin{pmatrix} -1 & 1 & 0 \\ -1 & 1 & 0 \\ 2 & -2 & 0 \end{pmatrix} \quad \text{and}$$
$$|v_{\mathbf{2A}}\rangle\langle v_{\mathbf{2S}}| = \frac{1}{\sqrt{12}}\begin{pmatrix} -1 & -1 & 2 \\ 1 & 1 & -2 \\ 0 & 0 & 0 \end{pmatrix}. \tag{A3}$$

If we define the tensors $\mathbf{T}_x^+ = |v_{\mathbf{2S}}\rangle\langle v_{\mathbf{2A}}| + |v_{\mathbf{2A}}\rangle\langle v_{\mathbf{2S}}|$ and $\mathbf{T}_x^- = i(|v_{\mathbf{2A}}\rangle\langle v_{\mathbf{2S}}| - |v_{\mathbf{2S}}\rangle\langle v_{\mathbf{2A}}|)$, we obtain

$$\mathbf{T}_x^+ = \frac{1}{\sqrt{3}}\begin{pmatrix} -1 & 0 & 1 \\ 0 & 1 & -1 \\ 1 & -1 & 0 \end{pmatrix} \quad \text{and}$$
$$\mathbf{T}_x^- = \frac{1}{\sqrt{3}}\begin{pmatrix} 0 & i & -i \\ -i & 0 & i \\ i & -i & 0 \end{pmatrix}. \tag{A4}$$

The terms proportional to the tensors $\mathbf{T}_x^+$ and $\mathbf{T}_x^-$ mix the components of the doublet representation with each other. Now,

$$|v_{\mathbf{1}}\rangle\langle v_{\mathbf{2}A}| = \frac{1}{\sqrt{6}}\begin{pmatrix} -1 & 1 & 0 \\ -1 & 1 & 0 \\ -1 & 1 & 0 \end{pmatrix} \quad \text{and}$$
$$|v_{\mathbf{2A}}\rangle\langle v_{\mathbf{1}}| = \frac{1}{\sqrt{6}}\begin{pmatrix} -1 & -1 & -1 \\ 1 & 1 & 1 \\ 0 & 0 & 1 \end{pmatrix}. \tag{A5}$$

If we define the tensors $\mathbf{T}_y^+ = |v_{\mathbf{1}}\rangle\langle v_{\mathbf{2A}}| + |v_{\mathbf{2A}}\rangle\langle v_{\mathbf{1}}|$ and $\mathbf{T}_y^- = i(|v_{\mathbf{2A}}\rangle\langle v_{\mathbf{2A}}| - |v_{\mathbf{2A}}\rangle\langle v_{\mathbf{2S}}|)$, we obtain

$$\mathbf{T}_y^+ = \frac{1}{\sqrt{6}}\begin{pmatrix} -2 & 0 & -1 \\ 0 & 2 & 1 \\ -1 & 1 & 0 \end{pmatrix} \quad \text{and}$$
$$\mathbf{T}_y^- = \frac{1}{\sqrt{6}}\begin{pmatrix} 0 & 2i & i \\ -2i & 0 & -i \\ -i & i & 0 \end{pmatrix}. \tag{A6}$$

The terms proportional to the tensors $\mathbf{T}_y^+$ and $\mathbf{T}_y^-$ mix the antisymmetric component of the doublet with the singlet. Finally,

$$|v_{\mathbf{1}}\rangle\langle v_{\mathbf{2S}}| = \frac{1}{3\sqrt{2}}\begin{pmatrix} 1 & 1 & -2 \\ 1 & 1 & -2 \\ 1 & 1 & -2 \end{pmatrix} \quad \text{and}$$
$$|v_{\mathbf{2S}}\rangle\langle v_{\mathbf{1}}| = \frac{1}{3\sqrt{2}}\begin{pmatrix} 1 & 1 & 1 \\ 1 & 1 & 1 \\ -2 & -2 & -2 \end{pmatrix}. \tag{A7}$$

If we define the tensors $\mathbf{T}_z^+ = |v_{\mathbf{1}}\rangle\langle v_{\mathbf{2S}}| + |v_{\mathbf{2S}}\rangle\langle v_{\mathbf{1}}|$ and $\mathbf{T}_y^- = i(|v_{\mathbf{2A}}\rangle\langle v_{\mathbf{2A}}| - |v_{\mathbf{2A}}\rangle\langle v_{\mathbf{2S}}|)$, then

$$\mathbf{T}_z^+ = \frac{1}{3\sqrt{2}}\begin{pmatrix} 2 & 2 & -1 \\ 2 & 2 & -1 \\ -1 & -1 & -4 \end{pmatrix} \quad \text{and}$$
$$\mathbf{T}_z^- = \frac{1}{\sqrt{2}}\begin{pmatrix} 0 & 0 & -i \\ 0 & 0 & -i \\ i & i & 0 \end{pmatrix}. \tag{A8}$$

The terms proportional to the tensors $\mathbf{T}_z^+$ and $\mathbf{T}_z^-$ mix the symmetric component of the doublet with the singlet. The tensor $\mathbf{T}_z^+$ can be written as a linear combination of two independent matrices,

$$\mathbf{T}_z^+ = \sqrt{\frac{2}{3}}\mathbf{T}_{z1}^+ - \frac{1}{3\sqrt{2}}\mathbf{T}_{z2}^+, \tag{A9}$$

where

$$\mathbf{T}_{z1}^+ = \begin{pmatrix} 1 & 1 & 0 \\ 1 & 1 & 0 \\ 0 & 0 & -2 \end{pmatrix} \quad \text{and}$$
$$\mathbf{T}_{z2}^+ = \begin{pmatrix} 0 & 0 & 1 \\ 0 & 0 & 1 \\ 1 & 1 & 0 \end{pmatrix}. \tag{A10}$$

APPENDIX B: CHENG-SHER PARAMETERS

$$\tilde{\mathbf{Y}}_k^{\mathrm{j}} = \mathbf{U}_{\mathrm{j}}^\dagger \mathbf{Y}_k^{\mathrm{w,j}} \mathbf{U}_{\mathrm{j}} = \mathbf{O}_{\mathrm{j}}^\top \mathbf{P}_{\mathrm{j}}^\dagger \mathbf{U}_{\mathrm{s}}^\dagger \mathbf{Y}_k^{\mathrm{w,j}} \mathbf{U}_{\mathrm{s}} \mathbf{P}_{\mathrm{j}} \mathbf{O}_{\mathrm{j}},$$
$$(\tilde{\mathbf{Y}}_k^{\mathrm{j}})_{\mathtt{rt}} = \frac{\sqrt{m_{\mathrm{j}\mathtt{r}} m_{\mathrm{j}\mathtt{s}}}}{v}(\tilde{\boldsymbol{\chi}}_k^{\mathrm{j}})_{\mathtt{rt}}, \qquad \mathtt{r},\mathtt{t} = 1,2,3, \tag{B1}$$

where

$$
\begin{aligned}
(\tilde{\boldsymbol{\chi}}_k^{\mathrm{j}})_{11} &= 2\frac{\xi_{\mathrm{J}1}}{D_{\mathrm{j}1}}\sqrt{\frac{\hat{m}_{\mathrm{j}2}}{\hat{m}_{\mathrm{j}1}}(1-\delta_{\mathrm{j}})}\cos(\phi_k^{\mathrm{j}}-\phi_{\mathrm{j}})\tilde{a}_k^{\mathrm{j}}+\frac{(1-\delta_{\mathrm{j}})\xi_{\mathrm{j}1}}{D_{\mathrm{j}1}}\tilde{b}_k^{\mathrm{j}}-2\frac{\sqrt{\delta_{\mathrm{j}}(1-\delta_{\mathrm{j}})\xi_{\mathrm{j}1}\xi_{\mathrm{j}2}}}{D_{\mathrm{j}1}}\tilde{c}_k^{\mathrm{j}}+\frac{\delta_{\mathrm{j}}\xi_{\mathrm{j}2}}{D_{\mathrm{j}1}}\tilde{d}_k^{\mathrm{j}},\\
(\tilde{\boldsymbol{\chi}}_k^{\mathrm{j}})_{12} &= \sqrt{\frac{(1-\delta_{\mathrm{j}})\xi_{\mathrm{j}1}\xi_{\mathrm{j}2}}{D_{\mathrm{j}1}D_{\mathrm{j}2}}}\left(\sqrt{\frac{\hat{m}_{\mathrm{j}2}}{\hat{m}_{\mathrm{j}1}}}e^{i(\phi_k^{\mathrm{j}}-\phi_{\mathrm{j}})}-\sqrt{\frac{\hat{m}_{\mathrm{j}1}}{\hat{m}_{\mathrm{j}2}}}e^{-i(\phi_k^{\mathrm{j}}-\phi_{\mathrm{j}})}\right)\tilde{a}_k^{\mathrm{j}}+(1-\delta\mathrm{j})\sqrt{\frac{\xi_{\mathrm{j}1}\xi_{\mathrm{j}2}}{D_{\mathrm{j}1}D_{\mathrm{j}2}}}\tilde{b}_k^{\mathrm{j}}-(\xi_{\mathrm{j}1}+\xi_{\mathrm{j}2})\sqrt{\frac{\delta_{\mathrm{j}}(1-\delta_{\mathrm{j}})}{D_{\mathrm{j}1}D_{\mathrm{j}2}}}\tilde{c}_k^{\mathrm{j}}\\
&\quad+\delta_{\mathrm{j}}\sqrt{\frac{\xi_{\mathrm{j}1}\xi_{\mathrm{j}2}}{D_{\mathrm{j}1}D_{\mathrm{j}2}}}\tilde{d}_k^{\mathrm{j}},\\
(\tilde{\boldsymbol{\chi}}_k^{\mathrm{j}})_{13} &= \sqrt{\frac{\hat{m}_{\mathrm{j}2}}{\hat{m}_{\mathrm{j}1}}\frac{(1-\delta_{\mathrm{j}})\delta_{\mathrm{j}}\xi_{\mathrm{j}1}}{D_{\mathrm{j}1}D_{\mathrm{j}3}}}(\hat{m}_{\mathrm{j}1}e^{-i(\phi_k^{\mathrm{j}}-\phi_{\mathrm{j}})}+e^{i(\phi_k^{\mathrm{j}}-\phi_{\mathrm{j}})})\tilde{a}_k^{\mathrm{j}}+(1-\delta_{\mathrm{j}})\sqrt{\frac{\delta_{\mathrm{j}}\xi_{\mathrm{j}1}}{D_{\mathrm{j}1}D_{\mathrm{j}3}}}\tilde{b}_k^{\mathrm{j}}+(\xi_{\mathrm{j}1}-\delta_{\mathrm{j}})\sqrt{\frac{(1-\delta_{\mathrm{j}})\xi_{\mathrm{j}2}}{D_{\mathrm{j}1}D_{\mathrm{j}3}}}\tilde{c}_k^{\mathrm{j}}\\
&\quad-\xi_{\mathrm{j}2}\sqrt{\frac{\delta_{\mathrm{j}}\xi_{\mathrm{j}1}}{D_{\mathrm{j}1}D_{\mathrm{j}3}}}\tilde{d}_k^{\mathrm{j}},\\
(\tilde{\boldsymbol{\chi}}_k^{\mathrm{j}})_{22} &= -2\sqrt{\frac{\hat{m}_{\mathrm{j}1}}{\hat{m}_{\mathrm{j}2}}(1-\delta_{\mathrm{j}})}\frac{\xi_{\mathrm{j}2}}{D_{\mathrm{j}2}}\cos(\phi_k^{\mathrm{j}}-\phi_{\mathrm{j}})\tilde{a}_k^{\mathrm{j}}+\frac{(1-\delta_{\mathrm{j}})\xi_{\mathrm{j}2}}{D_{\mathrm{j}2}}\tilde{b}_k^{\mathrm{j}}-2\frac{\sqrt{\delta_{\mathrm{j}}(1-\delta_{\mathrm{j}})\xi_{\mathrm{j}1}\xi_{\mathrm{j}2}}}{D_{\mathrm{j}2}}\tilde{c}_k^{\mathrm{j}}+\frac{\delta_j\xi_{\mathrm{j}}}{D_{\mathrm{j}2}}\tilde{d}_k^{\mathrm{j}},\\
(\tilde{\boldsymbol{\chi}}_k^{\mathrm{j}})_{23} &= -\sqrt{\frac{\hat{m}_{\mathrm{j}1}}{\hat{m}_{\mathrm{j}2}}\frac{\delta_{\mathrm{j}}(1-\delta_{\mathrm{j}})\xi_{\mathrm{j}2}}{D_{\mathrm{j}2}D_{\mathrm{j}3}}}(e^{i(\phi_k^{\mathrm{j}}-\phi_{\mathrm{j}})}-\hat{m}_{\mathrm{j}2}e^{-i(\phi_k^{\mathrm{j}}-\phi_{\mathrm{j}})})\tilde{a}_k^{\mathrm{j}}+(1-\delta_{\mathrm{j}})\sqrt{\frac{\delta_{\mathrm{j}}\xi_{\mathrm{j}2}}{D_{\mathrm{j}2}D_{\mathrm{j}3}}}\tilde{b}_k^{\mathrm{j}}+(\xi_{\mathrm{j}2}-\delta_{\mathrm{j}})\sqrt{\frac{(1-\delta_{\mathrm{j}})\xi_{\mathrm{j}1}}{D_{\mathrm{j}2}D_{\mathrm{j}3}}}\tilde{c}_k^{\mathrm{j}}\\
&\quad-\xi_{\mathrm{j}1}\sqrt{\frac{\delta_{\mathrm{j}}\xi_{\mathrm{j}2}}{D_{\mathrm{j}2}D_{\mathrm{j}3}}}\tilde{d}_k^{\mathrm{j}},\\
(\tilde{\boldsymbol{\chi}}_k^{\mathrm{j}})_{33} &= 2\sqrt{(1-\delta_{\mathrm{j}})\hat{m}_{\mathrm{j}1}\hat{m}_{\mathrm{j}2}}\frac{\delta_{\mathrm{j}}}{D_{\mathrm{j}3}}\cos(\phi_k^{\mathrm{j}}-\phi_{\mathrm{j}})\tilde{a}_k^{\mathrm{j}}+\frac{\delta_{\mathrm{j}}(1-\delta_{\mathrm{j}})}{D_{\mathrm{j}3}}\tilde{b}_k^{\mathrm{j}}+2\frac{\sqrt{\delta_{\mathrm{j}}(1-\delta_{\mathrm{j}})\xi_{\mathrm{j}1}\xi_{\mathrm{j}2}}}{D_{\mathrm{j}3}}\tilde{c}_k^{\mathrm{j}}+\frac{d_{\mathrm{jk}}\xi_{\mathrm{j}1}\xi_{\mathrm{j}2}}{D_{\mathrm{j}3}}\tilde{d}_k^{\mathrm{j}},
\end{aligned}
\tag{B2}
$$

with

$$
\tilde{a}_k^{\mathrm{j}}=\frac{v}{m_{\mathrm{j}3}}|A_k^{\mathrm{j}}|,\qquad \tilde{b}_k^{\mathrm{j}}=\frac{v}{m_{\mathrm{j}3}}B_k^{\mathrm{j}},\qquad \tilde{c}_k^{\mathrm{j}}=\frac{v}{m_{\mathrm{j}3}}C_k^{\mathrm{j}},\quad \text{and}\quad \tilde{d}_k^{\mathrm{j}}=\frac{v}{m_{\mathrm{j}3}}D_k^{\mathrm{j}}. \tag{B3}
$$

APPENDIX C: MIXING MATRIX

The lepton flavor-mixing matrix is

$$
\mathbf{U}_{\mathrm{PMNS}}=\mathbf{U}_l^{\dagger}\mathbf{U}_{\nu}=\mathbf{O}_l^{\top}\mathbf{P}_l^{\dagger}\mathbf{U}_{\mathrm{s}}^{\dagger}\mathbf{U}_{\mathrm{s}}\mathbf{P}_{\nu}\mathbf{O}_{\nu}^{\mathrm{n[i]}}=\mathbf{O}_l^{\top}\mathbf{P}^{(\nu-l)}\mathbf{O}_{\nu}^{\mathrm{n[i]}}. \tag{C1}
$$

The explicit forms of the entries of the previous matrix are

$$
\begin{aligned}
(\mathbf{U}_{\mathrm{PMNS}})_{11} &= \sqrt{\frac{\hat{m}_{\mu}\hat{m}_{\nu2[1]}\xi_{l1}\xi_{\nu1[3]}}{D_{l1}D_{\nu1[3]}}}+\sqrt{\frac{\hat{m}_e\hat{m}_{\nu1[3]}}{D_{l1}D_{\nu1[3]}}}\left(\sqrt{(1-\delta_{\nu})(1-\delta_l)\xi_{l1}\xi_{\nu1[3]}}e^{i\phi_{l1}}+\sqrt{\delta_{\nu}\delta_l\xi_{l2}\xi_{\nu2[1]}}e^{i\phi_{l2}}\right),\\
(\mathbf{U}_{\mathrm{PMNS}})_{12} &= -\sqrt{\frac{\hat{m}_{\mu}\hat{m}_{\nu1[3]}\xi_{l1}\xi_{\nu2[1]}}{D_{l1}D_{\nu2[1]}}}+\sqrt{\frac{\hat{m}_e\hat{m}_{\nu2[1]}}{D_{l1}D_{\nu2[1]}}}\left(\sqrt{(1-\delta_{\nu})(1-\delta_l)\xi_{l1}\xi_{\nu2[1]}}e^{i\phi_{l1}}+\sqrt{\delta_{\nu}\delta_l\xi_{l2}\xi_{\nu1[3]}}e^{i\phi_{l2}}\right),\\
(\mathbf{U}_{\mathrm{PMNS}})_{13} &= \sqrt{\frac{\hat{m}_{\mu}\hat{m}_{\nu1[3]}\hat{m}_{\nu2[1]}\delta_{\nu}\xi_{l1}}{D_{l1}D_{\nu3[2]}}}+\sqrt{\frac{\hat{m}_e}{D_{l1}D_{\nu3[2]}}}\left(\sqrt{(1-\delta_{\nu})\delta_{\nu}(1-\delta_l)\xi_{l1}}e^{i\phi_{l1}}-\sqrt{\delta_l\xi_{l2}\xi_{\nu1[3]}\xi_{\nu2[1]}}e^{i\phi_{l2}}\right),\\
(\mathbf{U}_{\mathrm{PMNS}})_{21} &= -\sqrt{\frac{\hat{m}_e\hat{m}_{\nu2[1]}\xi_{l2}\xi_{\nu1[3]}}{D_{l2}D_{\nu1[3]}}}+\sqrt{\frac{\hat{m}_{\mu}\hat{m}_{\nu1[3]}}{D_{l2}D_{\nu1[3]}}}\left(\sqrt{(1-\delta_{\nu})(1-\delta_l)\xi_{l2}\xi_{\nu1[3]}}e^{i\phi_{l1}}+\sqrt{\delta_{\nu}\delta_l\xi_{l1}\xi_{\nu2[1]}}e^{i\phi_{l2}}\right),
\end{aligned}
$$

$$
\begin{aligned}
(\mathbf{U}_{\mathrm{PMNS}})_{22} &= \sqrt{\frac{\tilde{m}_e \tilde{m}_{\nu 1[3]} \xi_{l2} \xi_{\nu 2[1]}}{D_{l2} D_{\nu 2[1]}}} + \sqrt{\frac{\tilde{m}_\mu \tilde{m}_{\nu 2[1]}}{D_{l2} D_{\nu 2[1]}}} \left(\sqrt{(1-\delta_\nu)(1-\delta_l)\xi_{l2}\xi_{\nu 2[1]}} e^{i\phi_{l1}} + \sqrt{\delta_\nu \delta_l \xi_{l1} \xi_{\nu 1[3]}} e^{i\phi_{l2}} \right), \\
(\mathbf{U}_{\mathrm{PMNS}})_{23} &= -\sqrt{\frac{\tilde{m}_e \tilde{m}_{\nu 1[3]} \tilde{m}_{\nu 2[1]} \delta_\nu \xi_{l2}}{D_{l2} D_{\nu 3[2]}}} + \sqrt{\frac{\tilde{m}_\mu}{D_{l2} D_{\nu 3[2]}}} \left(\sqrt{\delta_\nu (1-\delta_\nu)(1-\delta_l)\xi_{l2}} e^{i\phi_{l1}} - \sqrt{\delta_l \xi_{l1} \xi_{\nu 1[3]} \xi_{\nu 2[1]}} e^{i\phi_{l2}} \right), \\
(\mathbf{U}_{\mathrm{PMNS}})_{31} &= \sqrt{\frac{\tilde{m}_e \tilde{m}_\mu \tilde{m}_{\nu 2[1]} \delta_l \xi_{\nu 1[3]}}{D_{l3} D_{\nu 1[3]}}} + \sqrt{\frac{\tilde{m}_{\nu 1[3]}}{D_{l3} D_{\nu 1[3]}}} \left(\sqrt{\delta_l (1-\delta_\nu)(1-\delta_l)\xi_{\nu 1[3]}} e^{i\phi_{l1}} - \sqrt{\delta_\nu \xi_{l1} \xi_{l2} \xi_{\nu 2[1]}} e^{i\phi_{l2}} \right), \\
(\mathbf{U}_{\mathrm{PMNS}})_{32} &= -\sqrt{\frac{\tilde{m}_e \tilde{m}_\mu \tilde{m}_{\nu 1[3]} \delta_l \xi_{\nu 2[1]}}{D_{l3} D_{\nu 2[1]}}} + \sqrt{\frac{\tilde{m}_{\nu 2[1]}}{D_{l3} D_{\nu 2[1]}}} \left(\sqrt{\delta_l (1-\delta_\nu)(1-\delta_l)\xi_{\nu 2[1]}} e^{i\phi_{l1}} - \sqrt{\delta_\nu \xi_{l1} \xi_{l2} \xi_{\nu 1[3]}} e^{i\phi_{l2}} \right), \\
(\mathbf{U}_{\mathrm{PMNS}})_{33} &= \sqrt{\frac{\tilde{m}_e \tilde{m}_\mu \tilde{m}_{\nu 1[3]} \tilde{m}_{\nu 2[1]} \delta_l \delta_\nu}{D_{l3} D_{\nu 3[2]}}} + \sqrt{\frac{1}{D_{l3} D_{\nu 3[2]}}} \left(\sqrt{\delta_l \delta_\nu (1-\delta_\nu)(1-\delta_l)} e^{i\phi_{l1}} - \sqrt{\xi_{l1} \xi_{l2} \xi_{\nu 1[3]} \xi_{\nu 2[1]}} e^{i\phi_{l2}} \right).
\end{aligned} \tag{C2}
$$

[1] S. F. King, Unified models of neutrinos, flavour and *CP* violation, Prog. Part. Nucl. Phys. **94**, 217 (2017).

[2] F. Capozzi, E. Lisi, A. Marrone, D. Montanino, and A. Palazzo, Neutrino masses and mixings: Status of known and unknown 3ν parameters, Nucl. Phys. **B908**, 218 (2016).

[3] M. P. Decowski (KamLAND Collaboration), KamLAND's precision neutrino oscillation measurements, Nucl. Phys. **B908**, 52 (2016).

[4] A. Gando *et al.* (KamLAND Collaboration), Constraints on θ_{13} from a three-flavor oscillation analysis of reactor antineutrinos at KamLAND, Phys. Rev. D **83**, 052002 (2011).

[5] A. Gando *et al.* (KamLAND Collaboration), Reactor on-off antineutrino Measurement with KamLAND, Phys. Rev. D **88**, 033001 (2013).

[6] S.-H. Seo (RENO Collaboration), New results from RENO and the 5 MeV excess, AIP Conf. Proc. **1666**, 080002 (2015).

[7] J. H. Choi *et al.* (RENO Collaboration), Observation of energy and baseline dependent reactor antineutrino disappearance in the RENO experiment, Phys. Rev. Lett. **116**, 211801 (2016).

[8] Y. Abe *et al.* (Double Chooz Collaboration), Improved measurements of the neutrino mixing angle θ_{13} with the Double Chooz detector, J. High Energy Phys. 10 (2014) 086; Erratum, J. High Energy Phys. 02 (2015) 74.

[9] F. P. An *et al.* (Daya Bay Collaboration), Measurement of the Reactor Antineutrino Flux and Spectrum at Daya Bay, Phys. Rev. Lett. **116**, 061801 (2016); Erratum, Phys. Rev. Lett. **118**, 099902 (2017).

[10] G. J. Feldman, J. Hartnell, and T. Kobayashi, Long-baseline neutrino oscillation experiments, Adv. High Energy Phys. **2013**, 475749 (2013).

[11] K. Abe *et al.* (T2K Collaboration), Measurement of neutrino and antineutrino oscillations by the T2K experiment including a new additional sample of ν_e interactions at the far detector, Phys. Rev. D **96**, 092006 (2017).

[12] M. Batkiewicz (T2K Collaboration), Latest results from T2K, in *Proceedings of the 17th Lomonosov Conference on Elementary Particle Physics, Moscow, Russia, August 20–26, 2015*, edited by A. I. Studenikin (World Scientific, Singapore, 2017), p. 66.

[13] K. Abe *et al.* (T2K Collaboration), Combined analysis of neutrino and antineutrino oscillations at T2K, Phys. Rev. Lett. **118**, 151801 (2017).

[14] K. Abe *et al.* (T2K Collaboration), Measurements of neutrino oscillation in appearance and disappearance channels by the T2K experiment with 6.610^{20} protons on target, Phys. Rev. D **91**, 072010 (2015).

[15] L. Kolupaeva (NOνA Collaboration), Current results of the NOνA experiment, EPJ Web Conf. **125**, 01002 (2016).

[16] J. Bian (NOνA Collaboration), First results of ν_e appearance analysis and electron neutrino identification at NOνA, in *Proceedings of the Meeting of the APS Division of Particles and Fields (DPF 2015), Ann Arbor, Michigan, August 4–8, 2015* (to be published), arXiv:1510.05708.

[17] H. Wulandari, J. Jochum, W. Rau, and F. von Feilitzsch, Neutron flux at the Gran Sasso underground laboratory revisited, Astropart. Phys. **22**, 313 (2004).

[18] D. Forero, M. Tortola, and J. Valle, Neutrino oscillations refitted, Phys. Rev. D **90**, 093006 (2014).

[19] M. C. Gonzalez-Garcia, M. Maltoni, and T. Schwetz, Global analyses of neutrino oscillation experiments, Nucl. Phys. **B908**, 199 (2016).

[20] I. Esteban, M. C. Gonzalez-Garcia, M. Maltoni, I. Martinez-Soler, and T. Schwetz, Updated fit to three neutrino mixing: Exploring the accelerator-reactor complementarity, J. High Energy Phys. 01 (2017) 087.

[21] S.-F. Ge, Measuring the leptonic Dirac *CP* phase with TNT2K, in *Proceedings of NuPhys2016: Prospects in Neutrino Physics, London, UK, December 12–14, 2016* (to be published), arXiv:1704.08518.

[22] D. Atwood, L. Reina, and A. Soni, Phenomenology of two Higgs doublet models with flavor changing neutral currents, Phys. Rev. D **55**, 3156 (1997).

[23] J. L. Diaz-Cruz, J. Hernández-Sánchez, S. Moretti, R. Noriega-Papaqui, and A. Rosado, Yukawa textures and charged Higgs boson phenomenology in the 2HDM-III, Phys. Rev. D **79**, 095025 (2009).

[24] J. L. Diaz-Cruz, R. Noriega-Papaqui, and A. Rosado, Measuring the fermionic couplings of the Higgs boson at future colliders as a probe of a non-minimal flavor structure, Phys. Rev. D **71**, 015014 (2005).

[25] M. Krawczyk and D. Sokolowska, The charged Higgs boson mass in the 2HDM: Decoupling and CP violation, in *Presented at 2007 International Linear Collider Workshop (LCWS07 and ILC07)*, eConf C0705302, HIG09 (2007).

[26] J. E. Barradas Guevara, F. Cázarez Bush, A. Cordero Cid, O. Félix Beltrán, J. Hernández Sánchez, and R. Noriega Papaqui, Implications of Yukawa textures in the decay $H^+ \to W^+\gamma$ within the 2HDM-III, J. Phys. G **37**, 115008 (2010).

[27] A. Crivellin, A. Kokulu, and C. Greub, Flavor-phenomenology of two-Higgs-doublet models with generic Yukawa structure, Phys. Rev. D **87**, 094031 (2013).

[28] M. Krawczyk, Testing Higgs sector of 2HDM, *Proc. Sci.*, HEP2005 (2006) 335 [arXiv:hep-ph/0512371].

[29] G. C. Branco, P. M. Ferreira, L. Lavoura, M. N. Rebelo, M. Sher, and J. P. Silva, Theory and phenomenology of two-Higgs-doublet models, Phys. Rep. **516**, 1 (2012).

[30] F. F. Deppisch, Lepton flavour violation and flavour symmetries, Fortschr. Phys. **61**, 622 (2013).

[31] I. Dorsner and S. M. Barr, Flavor exchange effects in models with Abelian flavor symmetry, Phys. Rev. D **65**, 095004 (2002).

[32] H. Georgi, Lie Algebras in Particle Physics, Front. Phys. **54**, 1 (1999).

[33] H. Ishimori *et al.*, Non-abelian discrete symmetries in particle physics, Prog. Theor. Phys. Suppl. **183**, 1 (2010).

[34] C. Patrignani *et al.* (Particle Data Group), Review of particle physics, Chin. Phys. C **40**, 100001 (2016).

[35] Z.-z. Xing, Neutrino masses, and flavor mixing, Nucl. Phys. B, Proc. Suppl. **203**, 82 (2010).

[36] A. Das and N. Okada, Inverse seesaw neutrino signatures at the LHC and ILC, Phys. Rev. D **88**, 113001 (2013).

[37] A. Das and N. Okada, Bounds on heavy Majorana neutrinos in type-I seesaw and implications for collider searches, Phys. Lett. B **774**, 32 (2017).

[38] E. Barradas-Guevara *et al.*, Analysis of the lepton mixing matrix in the two Higgs doublet model, JNPMSRA **4**, 203 (2016).

[39] W. Wang and Z.-L. Han, Global $U(1)_L$ breaking in neutrinophilic 2HDM: From LHC signatures to x-ray line, Phys. Rev. D **94**, 053015 (2016).

[40] O. Felix-Beltran, F. González-Canales, J. Hernández-Sánchez, S. Moretti, R. Noriega-Papaqui, and A. Rosado, Analysis of the quark sector in the 2HDM with a four-zero Yukawa texture using the most recent data on the CKM matrix, Phys. Lett. B **742**, 347 (2015).

[41] F. Gonzalez Canales, A. Mondragon, and M. Mondragon, The S_3 flavour symmetry: Neutrino masses and mixings, Fortschr. Phys. **61**, 546 (2013).

[42] F. González Canales, A. Mondragón, M. Mondragón, U. J. Saldaña Salazar, and L. Velasco-Sevilla, Quark sector of S_3 models: Classification and comparison with experimental data, Phys. Rev. D **88**, 096004 (2013).

[43] J. Barranco, F. Gonzalez Canales, and A. Mondragon, Universal mass texture, CP violation and quark-lepton complementarity, Phys. Rev. D **82**, 073010 (2010).

[44] A. Mondragón and E. Rodríguez-Jáuregui, Breaking of the flavor permutational symmetry: Mass textures and the CKM matrix, Phys. Rev. D **59**, 093009 (1999).

[45] T. Cheng and M. Sher, Mass matrix ansatz and flavor nonconservation in models with multiple Higgs doublets, Phys. Rev. D **35**, 3484 (1987).

[46] J. L. Diaz-Cruz, R. Noriega-Papaqui, and A. Rosado, Mass matrix ansatz and lepton flavor violation in the THDM-III, Phys. Rev. D **69**, 095002 (2004).

[47] J. Hernandez-Sanchez, S. Moretti, R. Noriega-Papaqui, and A. Rosado, Update of the 2HDM-III with a four-zero texture in the Yukawa matrices and phenomenology of the charged Higgs boson, *Proc. Sci.*, CHARGED2012 (2012) 029 [arXiv:1302.0083].

[48] M. Gomez-Bock, G. Lopez Castro, L. Lopez-Lozano, and A. Rosado, Flavor-changing neutral current in production and decay of pseudoscalar mesons in a type III two-Higgs-doublet-model with four-texture Yukawa couplings, Phys. Rev. D **80**, 055017 (2009).

[49] R. Martinez, J. A. Rodriguez, and S. Sanchez, Charged Higgs production at photon colliders in 2HDM-III, Braz. J. Phys. **38**, 507 (2008).

[50] R. Martinez, J. A. Rodriquez, and D. A. Milanes, The lightest Higgs boson production at photon colliders in the 2HDM-III, Phys. Rev. D **72**, 035017 (2005).

[51] K. A. Hochmuth, S. T. Petcov, and W. Rodejohann, $u_{\rm pmns} = u_l^\dagger u_\nu$, Phys. Lett. B **654**, 177 (2007).

[52] S. Bilenky, *Introduction to the Physics of Massive and Mixed Neutrinos* (Springer, Berlin, Heidelberg, 2010).

[53] G. C. Branco, L. Lavoura, and M. N. Rebelo, Majorana neutrinos and CP violation in the leptonic sector, Phys. Lett. B **180**, 264 (1986).

[54] G. C. Branco, R. G. Felipe, and F. R. Joaquim, Leptonic CP violation, Rev. Mod. Phys. **84**, 515 (2012).

[55] E. E. Jenkins and A. V. Manohar, Rephasing invariants of quark and lepton mixing matrices, Nucl. Phys. **B792**, 187 (2008).

[56] P. A. R. Ade *et al.* (Planck Collaboration), Planck 2015 results. XIII. Cosmological parameters, Astron. Astrophys. **594**, A13 (2016).

[57] J. Schechter and J. W. F. Valle, Neutrinoless double beta decay in $SU(2) \times U(1)$ Theories, Phys. Rev. D **25**, 2951 (1982).

[58] M. Duerr, M. Lindner, and A. Merle, On the quantitative impact of the Schechter-Valle theorem, J. High Energy Phys. 06 (2011) 091.

[59] J. Beringer *et al.* (Particle Data Group), Review of particle physics (RPP), Phys. Rev. D **86**, 010001 (2012).

[60] V. Barger, D. Marfatia, and A. Tregre, Neutrino mass limits from SDSS, 2dFGRS and WMAP, Phys. Lett. B **595**, 55 (2004).

[61] S. F. King, A. Merle, and A. J. Stuart, The power of neutrino mass sum rules for neutrinoless double beta decay experiments, J. High Energy Phys. 12 (2013) 005.

[62] J. Schechter and J. W. F. Valle, Neutrino masses in $su(2) \times u(1)$ theories, Phys. Rev. D **22**, 2227 (1980).

[63] P. Chen, G.-J. Ding, F. Gonzalez-Canales, and J. W. F. Valle, Generalized $\mu - \tau$ reflection symmetry and leptonic *CP* violation, Phys. Lett. B **753**, 644 (2016).

[64] M. Auger *et al.* (EXO-200 Collaboration), Search for neutrinoless double-beta decay in ^{136}Xe with EXO-200, Phys. Rev. Lett. **109**, 032505 (2012).

[65] J. B. Albert *et al.* (EXO-200 Collaboration), Search for Majorana neutrinos with the first two years of EXO-200 data, Nature (London) **510**, 229 (2014).

[66] A. Gando *et al.* (KamLAND-Zen Collaboration), Limit on neutrinoless $\beta\beta$ decay of ^{136}Xe from the first phase of KamLAND-Zen and comparison with the positive claim in ^{76}Ge, Phys. Rev. Lett. **110**, 062502 (2013).

[67] M. V. Diwan, V. Galymov, X. Qian, and A. Rubbia, Long-baseline neutrino experiments, Annu. Rev. Nucl. Part. Sci. **66**, 47 (2016).

[68] K. Abe *et al.* (T2K Collaboration), The T2K experiment, Nucl. Instrum. Methods Phys. Res., Sect. A **659**, 106 (2011).

[69] P. Adamson *et al.* (NOνA Collaboration), First measurement of electron neutrino appearance in NOνA, Phys. Rev. Lett. **116**, 151806 (2016).

[70] R. Acciarri *et al.* (DUNE Collaboration), Long-Baseline Neutrino Facility (LBNF) and Deep Underground Neutrino Experiment (DUNE), arXiv:1512.06148.

[71] H. Nunokawa, S. Parke, and J. W. Valle, *CP* violation and neutrino oscillations, Prod. Part. Nucl. Phys. **60**, 338 (2008).

[72] F. Gonzalez-Canales, The remnant *CP* transformation and its implications, J. Phys. Conf. Ser. **761**, 012046 (2016).